

LUT UNIVERSITY  
LUT School of Energy Systems  
LUT Mechanical Engineering

*Mikael Paavolainen*

**ANALYSIS OF BALE CLAMP FRAME**

4.10.2021

Examiner(s): Professor Timo Björk  
M. Sc. (Tech.) Jari Virtanen

## **SAMMANFATTNING**

LUT-Yliopisto  
LUT School of Energy Systems  
LUT Kone

Mikael Paavolainen

### **Balpressens stams analys**

Diplomarbete

2021

56 sidor, 55 bilder, 11 tabeller ja 7 tillägg

Granskare: Professor Timo Björk  
DI Jari Virtanen

Nyckelord: balpress, FE-analys, plåts styvning

Dessa diplomarbetets objektiv var att ta reda på om man kan öka balpressens kapacitet. Dessa var gjord genom att ta reda på var är det mest kritiska stället i strukturen. När det kritiska stället hittades gjordes några förändringar för strukturen. Fyra olika belastningsfall analyserades som Auramo gav. Analysen gjordes med hjälp av FE-analys.

Litteraturgranskningen fokuserades på att förklara metoderna och ekvationerna som användes i räkningarna. Största fokusen var i modelleringen och att få FE-analysen att funka rätt. Metoderna som användes var Hot Spot och några Eurocode 3 ekvationer. Statiska kapaciteten analyserade men den större risken var i utnötningen av strukturen.

Resultaten visade att det kritiska stället var vid cylinder hållaren. Utnötningen skulle hända vid svets tån av cylinder hållaren. Förändringarna som gjordes för strukturen var att man lade till material vid cylinderhållarna och svetsa där ett styvnings plåt. Spänningarna vid cylinderhållarna orsakades mest av böjning. Med svetsningen av styvningsplåtarna förminskade spänningarna mycket och risken för utmatning blev mindre.

## **ABSTRACT**

LUT University  
LUT School of Energy Systems  
LUT Mechanical Engineering

Mikael Paavolainen

### **Analysis of bale clamp frame**

Master's thesis

2021

56 pages, 55 figures, 11 tables and 7 appendices

Examiners: Professor Timo Björk  
M. Sc. (Tech.) Jari Virtanen

Keywords: FEA, bale clamp, plate bending, FE-analysis

The objective of this master's thesis was to find out if the capacity of a bale clamp can be increased. This was done by finding out the most critical point in the structure. When the critical points were found, some improvements were done for the structure. Four different loading cases were analyzed which were provided by Auramo. The analysis of the loading cases was done using FE-analysis.

The literature review was focused on explaining the methods and equations used for the calculations. The biggest focus was on the modelling and getting the FE-model working properly. The used methods were Hot Spot-method and some Eurocode 3 equations for bolted connections. The static durability was investigated but the risk of failure through fatigue was bigger.

The results showed that the critical point in the structure is the cylinder bracket. The fatigue failure would occur by the cylinder bracket weld toe. The improvements for the structure were adding material by the cylinder bracket and adding a stiffener plate to reduce the stresses by the bracket. The stresses by the bracket were mostly caused by bending. Adding the stiffener reduced the stresses a lot and made the structure more durable and the risk for fatigue failure smaller.

## ACKNOWLEDGEMENTS

I want to thank you Auramo for providing this interesting master's thesis subject. I also want to thank you examiners M. Sc. Jari Virtanen and professor Timo Björk for the guidance during the process of writing the thesis.

Lastly, I want to thank my family for supporting me during my studies and a special thank you I want to say for my grandparents. Their help and support before my studies at LUT University has been irreplaceable.

*Mikael Paavolainen*

Mikael Paavolainen

Vantaa 4.10.2021

## TABLE OF CONTENTS

### SAMMANFATTNING

### ABSTRACT

### ACKNOWLEDGEMENTS

### TABLE OF CONTENTS

### LIST OF SYMBOLS AND ABBREVIATIONS

<b>1</b>	<b>INTRODUCTION .....</b>	<b>9</b>
	1.1 Background and motivation.....	9
	1.2 Aims of the study.....	10
	1.3 Research questions.....	10
	1.4 Limitations .....	11
<b>2</b>	<b>PRELIMINARY ANALYSES.....</b>	<b>12</b>
	2.1 Initial data for analyses .....	12
	2.2 Solidworks model .....	15
	2.3 FE-model .....	17
	2.3.1 Loads.....	17
	2.3.2 Constraints .....	19
	2.3.3 Bolted connection .....	21
	2.3.4 Mesh.....	23
	2.4 Results from the preliminary analyses.....	24
	2.4.1 Bolt forces.....	32
<b>3</b>	<b>IMPROVMENTS FOR THE STRUCTURE.....</b>	<b>35</b>
<b>4</b>	<b>FINAL ANALYSES.....</b>	<b>38</b>
	4.1 Mesh.....	38
	4.2 Constraints .....	39
	4.3 Fatigue life calculations .....	40
	4.3.1 Hot Spot method .....	40
	4.3.2 Calculating the fatigue life.....	43
	4.4 Results from final analyzes.....	44
	4.4.1 Bolt forces.....	48
	4.5 Fatigue life results.....	49

4.5.1	Frame plate fatigue life results.....	49
4.5.2	Bolt fatigue life results.....	52
<b>5</b>	<b>DISCUSSION .....</b>	<b>53</b>
<b>6</b>	<b>SUMMARY .....</b>	<b>55</b>
	<b>LIST OF REFERENCES.....</b>	<b>56</b>

## **APPENDIX**

Appendix I: Original structure, bolt forces

Appendix II: Modified structure, bolt forces

Appendix III: Mathcad base for Hot Spot, cylinder bracket, only clamping

Appendix IV: Mathcad base for Hot Spot, frame plate, only clamping

Appendix V: Mathcad base for Hot Spot, cylinder bracket, clamping and lifting

Appendix VI: Mathcad base for Hot Spot, frame plate, clamping and lifting

Appendix VII: Fatigue life calculations for bolts, LC2

## LIST OF SYMBOLS AND ABBREVIATIONS

$A_s$	Tensile strength area of the bolt
$E$	Modulus of elasticity [GPa]
$E_p$	Bale distance from arm backplates
$F_\mu$	Friction force [N]
$F_c$	Cylinder force [N]
$F_Q$	Force caused by pallet weight [N]
$F_{v,Rd}$	Design shear resistance per bolt
$F_{t,Rd}$	Design tension resistance per bolt
$f_{ub}$	Ultimate tensile strength
$\gamma_{M2}$	Partial safety factor for bolted connection
$g$	Acceleration caused by gravity
$K$	Arm outer distance measure [mm]
$N_D$	Calculated number of life cycles
$\mu$	Friction coefficient
$P_f$	Distance of resultant force of clamp [mm]
$P_q$	Distance of load center of gravity [mm]
$Q$	Load weight [kg]
$R_m$	Tensile strength [MPa]
$\sigma_b$	Bending stress [MPa]
$\sigma_{hs}$	Structural stress [MPa]
$\sigma_m$	Membrane stress [MPa]
$\sigma_{nl}$	Nonlinear stress peak [MPa]
$t$	Plate thickness [mm]
$\nu$	Poisson's ratio [-]
ENS	Effective Notch Stress
FAT	Fatigue class
FEM	Finite element method
HS	Hot Spot

IIW      International Institute of Welding  
LC      Loading case

## 1 INTRODUCTION

This master's thesis was done for Auramo Oy which is located in Järvenpää, Finland. Auramo Oy is a part of the Bolzoni concern which makes Bolzoni Auramo and Meyer forklift attachments. They are one of the leading forklift fork and attachment manufacturers in the world. They also provide maintenance services.

### 1.1 Background and motivation

Auramo has a bale clamp which is used as an attachment in forklifts. Their model B-400 is used for lifting and handling pulp and wastepaper bales. The bales are clamped between the arms of the bale clamp. The force is conducted using hydraulic cylinders. The load is lifted using friction force. The current maximum capacity of the B-400 model is 4000 kg. The B-400 bale clamp model is presented in figure 1.



**Figure 1.** B-400 bale clamp (Bolzoni Group 2020).

The bale clamp consists of a frame plate made of steel where is welded two stiffeners, and then two aluminum profiles which are attached using hex bolts. The hydraulics are attached to the frame plate using cylinder brackets that are welded on the plate. The B-400 model without the arms and hydraulics are presented in figure 2.

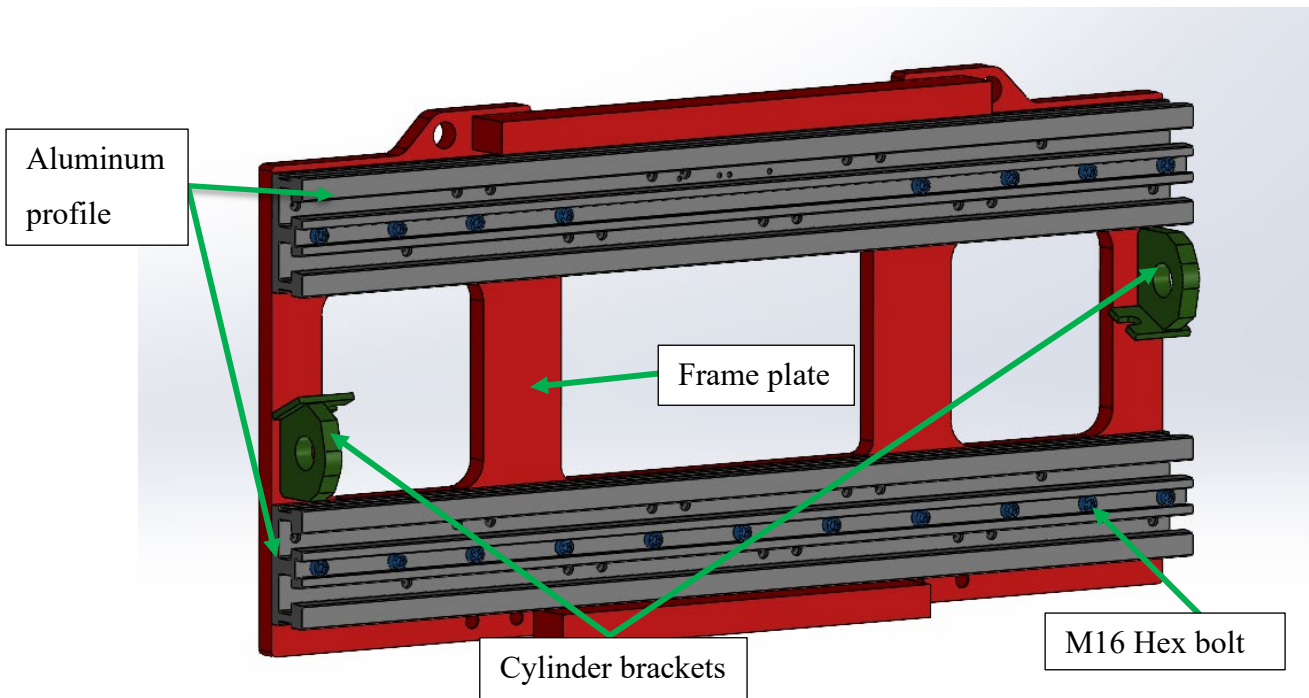


**Figure 2.** B-400 without arms and hydraulics.

The next model with a bigger capacity has steel profiles instead of aluminum. Auramo wants to see if the capacity can be increased using the aluminum profiles due them being cheaper to manufacture than the steel ones. The weight of the structure is also much lighter when using the aluminum profiles.

### 1.2 Aims of the study

The aims in this study are to find out if the capacity of the B-400 model can be increased with some adjustments when using the aluminum profiles. The task to find a way to increase the capacity by possibly modifying the frame plate dimensions with the given limitations and finding the limiting factor of increasing the capacity. The bale clamp is analyzed using FEM (Finite Element Method) and using analytical equations. There will be some things that brings uncertainty in the results. There can be combinations of loadings during operation that cannot be analyzed. The loading is also dependent a lot of in what position the arms are.

### 1.3 Research questions

The main objective is to find out the possibility to increase the capacity using the steel frame and aluminum profile combination. The other objective is to find out what sets the limit for

increasing the capacity. The objective is also to find out what is the critical component for the structure. Is it the bolt connections, aluminum profiles or the steel frame?

The research questions are:

- Can the capacity be increased?
- What is the limiting factor in increasing the capacity?
- How can the bale clamp be strengthened within the limitations?

#### 1.4 Limitations

This study is limited to the study of the frame, the aluminum profiles, and the bolt connections. The arms are only included in applying the load, so they are not analyzed more specifically. The materials are also predefined. There are some limitations regarding the dimensions. The frame plate height can be changed but not the width.

## 2 PRELIMINARY ANALYSES

The first step is to find out where is the critical point for the bale clamp. This is done using FE-analysis. Auramo provided some initial data which include four different loading cases. The initial data is presented in chapter 2.1. These four cases will be analyzed and from the results we can look where the critical point of the structure is. The analyses will be done using Solidworks FEA. The assembly is complex with many different parts so modelling it with e.g. FEMAP it would take too much time only to find the most critical loading case. This is the most effective way timewise. Solidworks is also widely used by companies that specialize 3D designs that also requires FE-analysis. The differences between Solidworks FEA and Femap is small, and the difference is not so big that it would make difference in the study of the bale clamp. There has been done a bachelors thesis where the differences between Solidworks FEA and Femap was studied. It should be taken to account that the mesh should be enough fine on the spots where the biggest stresses are at. (Matikainen, 2013, p. 39-40.)

### 2.1 Initial data for analyses

The preliminary analyses are done using preliminary loading cases that are provided by Auramo. There are four different loading cases where some parameters are changing. The loading cases are presented below in table 1.

*Table 1. Loading cases (Virtanen 2021).*

Loading case	$P_q$ [mm]	$P_f$ [mm]	$E_p$ [mm]	Operation
LC1	900	900	0	Clamping, lifting
LC2	1200	1050	300	Clamping, lifting
LC3	0	1440	1080	Clamping
LC4	0	1620	1440	Clamping

In table 1  $Q$  is the weight of the pallet,  $P_q$  center of gravity of the load,  $E_p$  is the distance of the pallet edge,  $P_f$  is the resultant force caused by the clamping and  $F_\mu$  is the friction force between the aluminum profile and the T-profile of the arms the locations are presented later in the figures. The point from where the dimensions are measured for the values in table 1 are presented below in figure 3. A dynamic factor of 1.3 will also be applied on the load. The used gravitational constant is  $g = 9.81 \text{ m/s}^2$ . The total force caused by the pallet weight with dynamic constant included can be calculated as follows.

$$F_Q = Q \times 1.3 \times g \quad (1)$$

where  $F_Q$  = total force caused by pallet weight  
 $Q$  = pallet weight  
 $g$  = acceleration caused by gravity

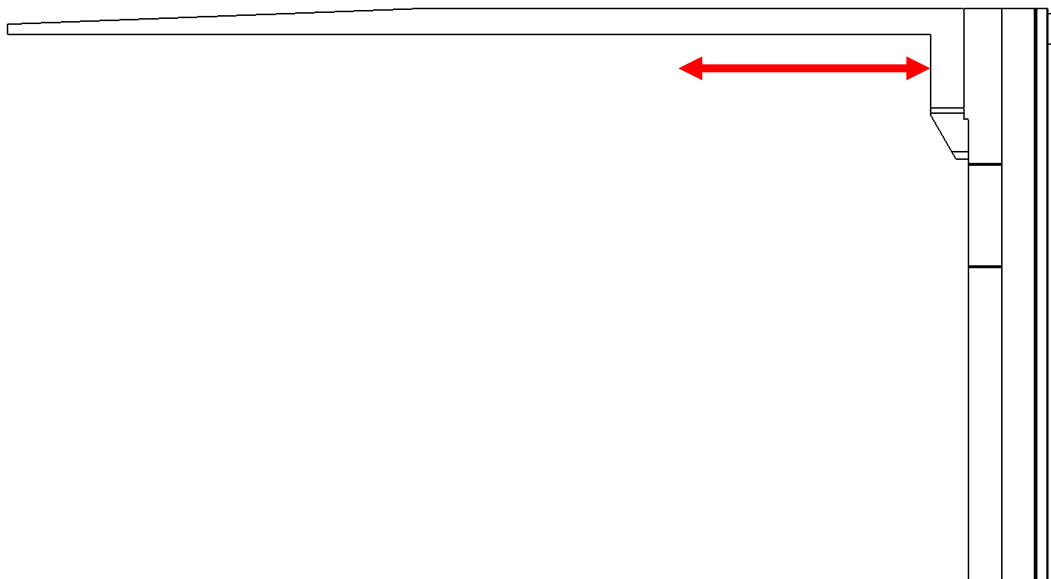


**Figure 3.** Measuring point in the arm for the loading cases (red arrow).

The material used in the bale clamp is S355 except the profiles are made from aluminum. The material properties used for the analyses are presented below in table 2.

Table 2. Material properties for FEA analysis.

	S355	Aluminum
$E$	210 GPa	70 GPa
$\nu$	0.3	0.3
$\rho$	7850 kg/m <sup>3</sup>	2700 kg/m <sup>3</sup>

In table 2  $E$  is modulus of elasticity,  $\nu$  is poisson's ratio and  $\rho$  is material density. The range the arms can move sideways is  $K = 670 \dots 2640$  mm. This is when not loaded and then when the arms are loaded the range is  $K = 670 \dots 2300$  mm. The arm moving range is presented below in figure 4.

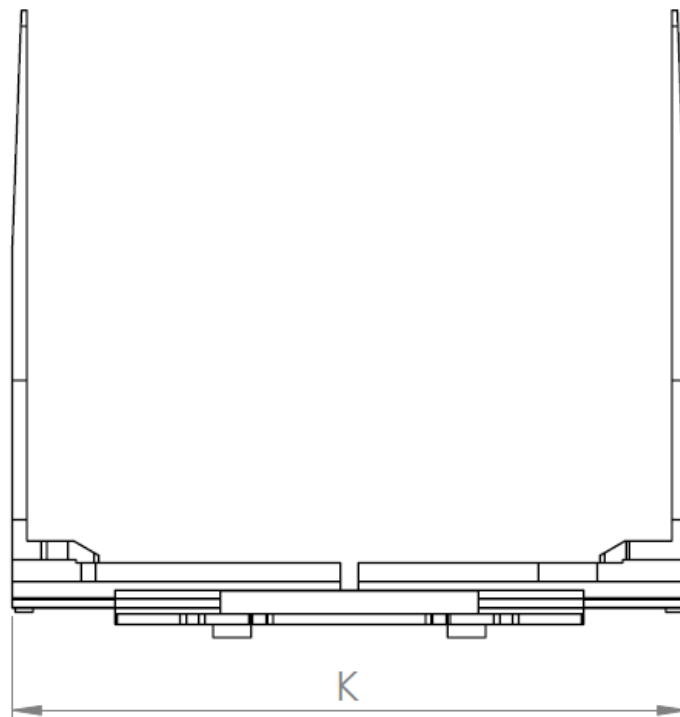
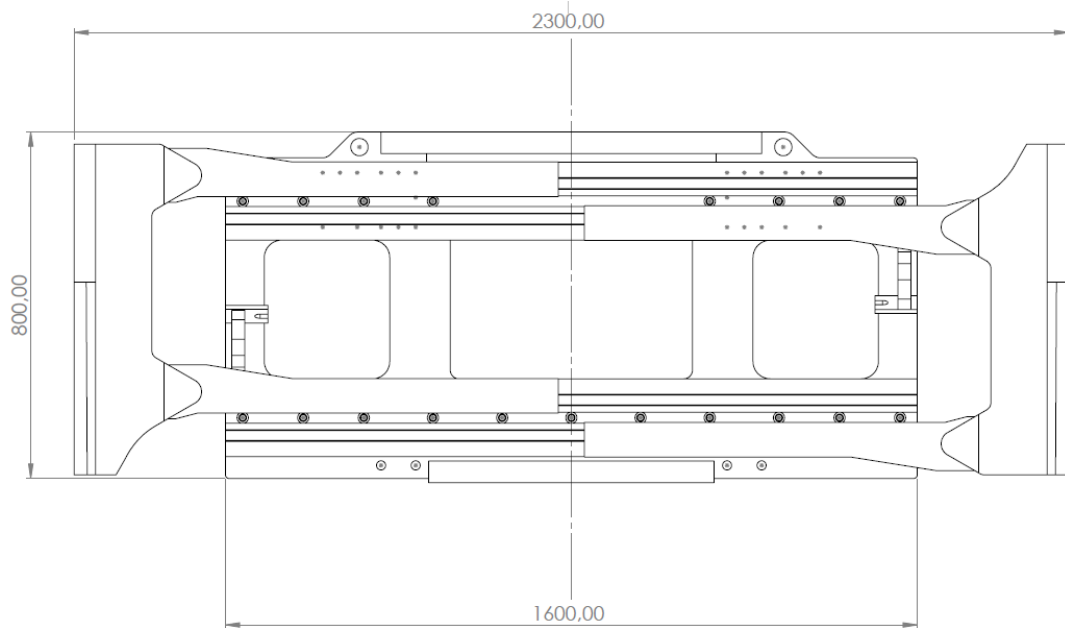


Figure 4. Arm moving range.

The used bolts in the assembly to fasten the aluminum profiles to the frame plate are M16 strength class 12.9 hex bolts. There are 8 bolts on the upper profile and 11 on the lower one. The bolts minimum tensile strength  $R_m$  is 1220 MPa. (SFS EN ISO 898-1. 2013. p. 8) The bolts are fastened with a tightening torque of 175 Nm.

## 2.2 Solidworks model

The 3D-models were provided by Auramo but they were in STEP-format and it was hard to make adjustments to them, so the frame plate was modelled using Solidworks from scratch. The main dimensions of the assembly are presented below in figure 5 and 6.



**Figure 5.** Bale clamp main dimensions [mm].

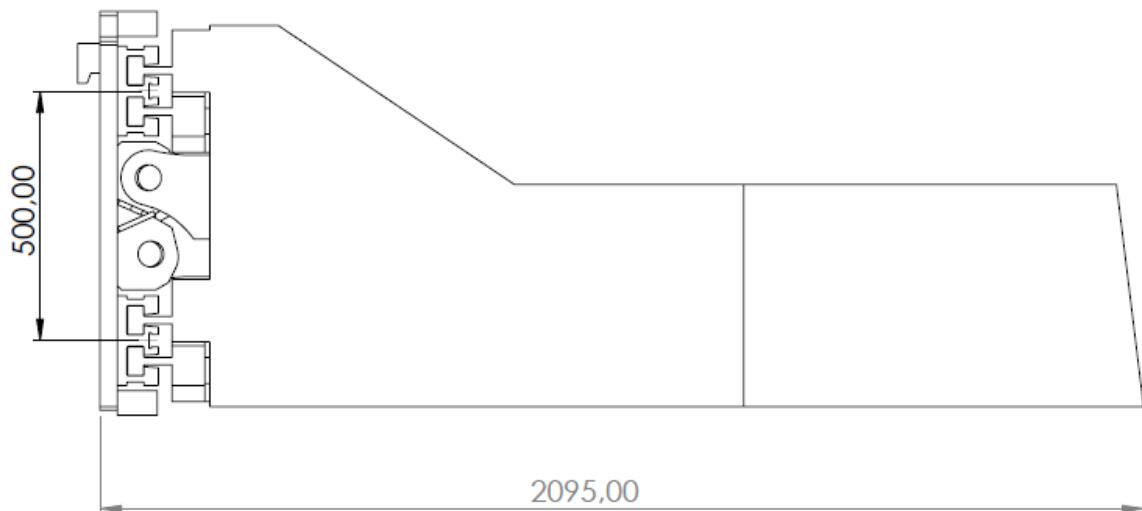


**Figure 6.** Bale clamp main dimensions [mm].

For the FE-analysis some split lines are needed for applying the constraints and loads. These are:

- On the arms for the area that is clamping the pallet
- Where the vertical load  $F_Q$  of the pallet is applied
- Back of the frame plate where the contact would be on the carriage

Split lines and the dimensions are presented below in figure 7 and 8.

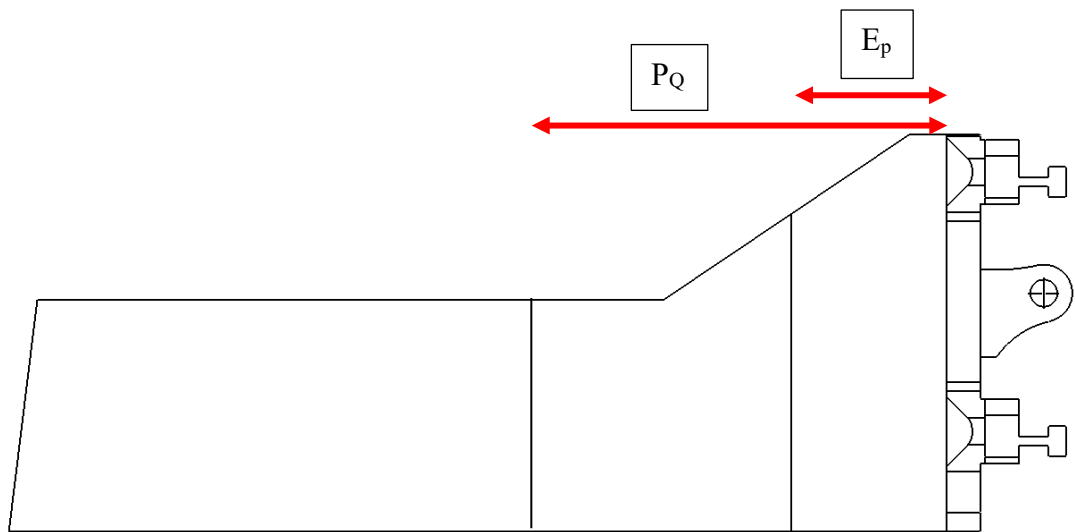


**Figure 7.** Arm split lines for FE- analysis constraints.

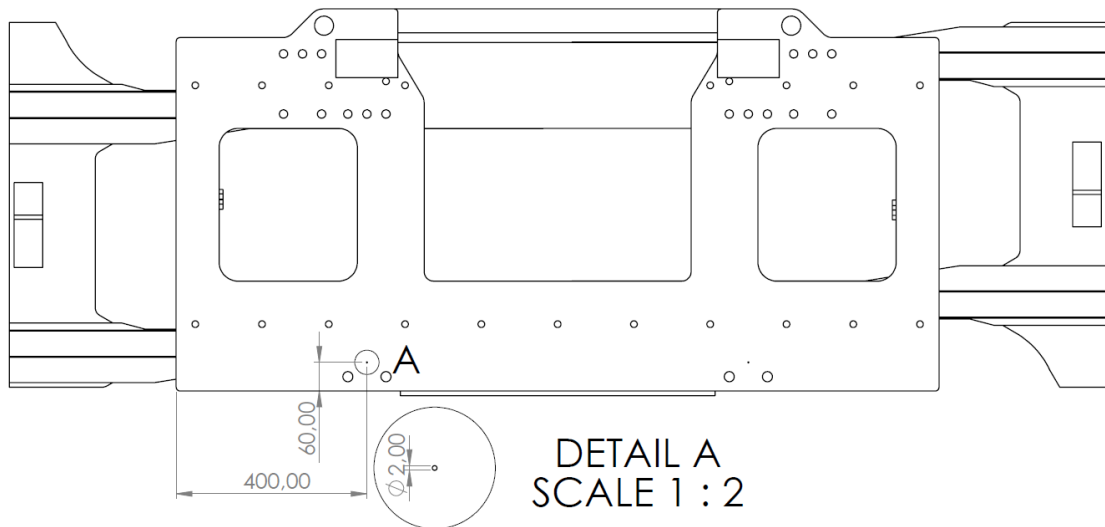


**Figure 8.** Frame plate split lines.

There would be in a real case hooks at the holes below the split lines, but they will not be included in the model because they are not loaded in normal use. Below in figure 9 is the full model of the bale clamp.

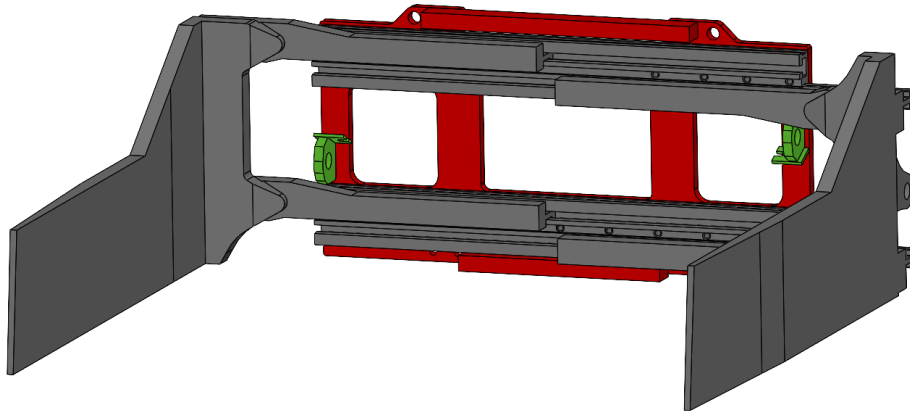


**Figure 9.** Bale clamp.

### 2.3 FE-model

The FE-analysis is done using Solidworks own FEA. The solver used in these analyses is direct sparse. The FEA is integrated to Solidworks so no importing files anywhere is needed. The assembly is taken to FEA without the modelled M16 hex bolts. The bolts are defined in the FEA, so no solid models are needed for them.

#### 2.3.1 Loads

There are four different kinds of loads used in the analyses depending on the loading case. The loads are friction force  $F_{\mu}$  between the T-profiles and the aluminum profile, cylinder force  $F_c$  and the load caused by the pallet weight  $F_Q$ . The loads used in the preliminary analyses are shown earlier in table 1. The places where the loads are applied is presented below in figure 10, 11 and 12.

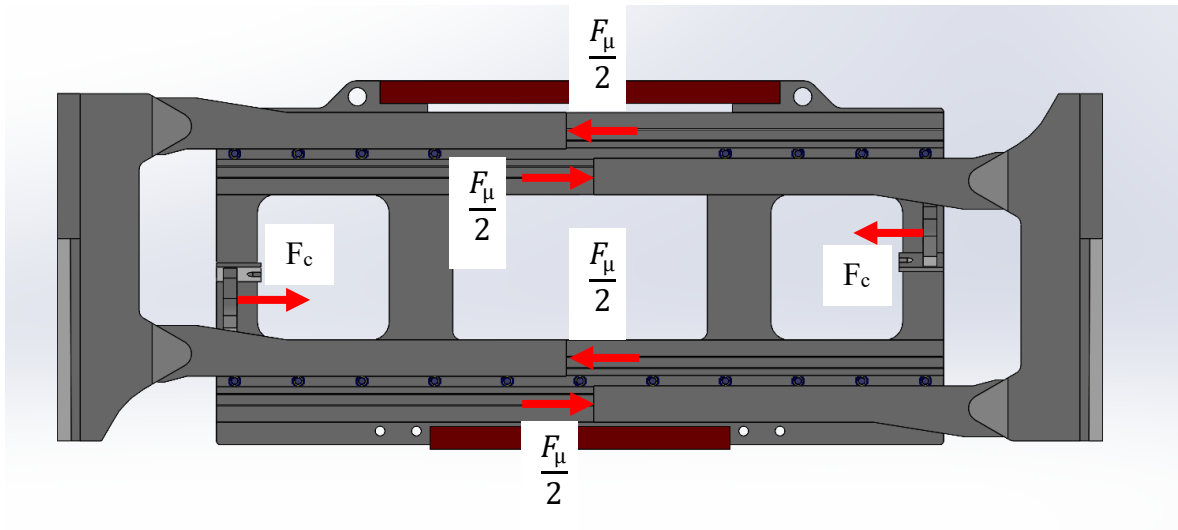


**Figure 10.** Loads applied on the model.

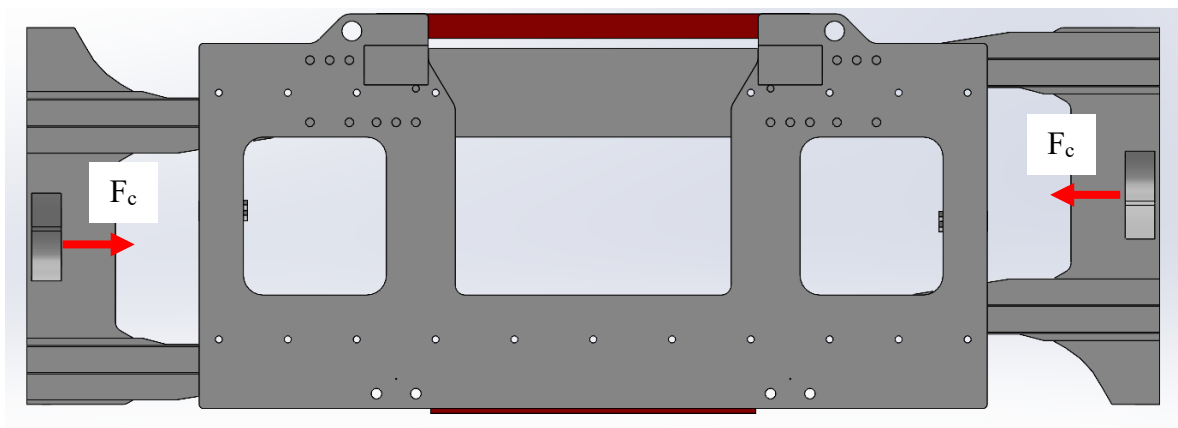


**Figure 11.** Loads applied on the model, back view.

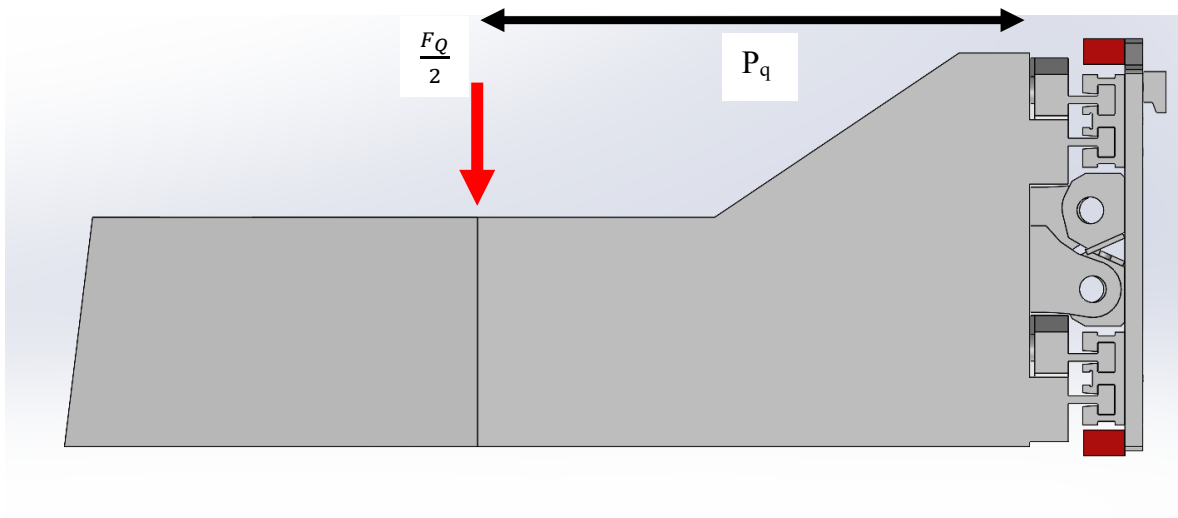


**Figure 12.** Load applied on the model, side view.

### 2.3.2 Constraints

In Solidworks the constraints are applied on the geometry lines and therefore we previously added the split lines for the model. The frame plate is constrained 30 mm above and between the holes where the bottom hooks would be in a real case. The 30 mm above is the place where the frame plate would touch the carriage where the bale clamp is fastened. This will be a point constrain so that the frame plate can deform as realistically as possible. If the constraint would be all the way through the width of the plate the results would not be liable. The frame plate at this location is constrained so that all translations along Z-axis are prevented. The constrain applied can be seen below in figure 13.

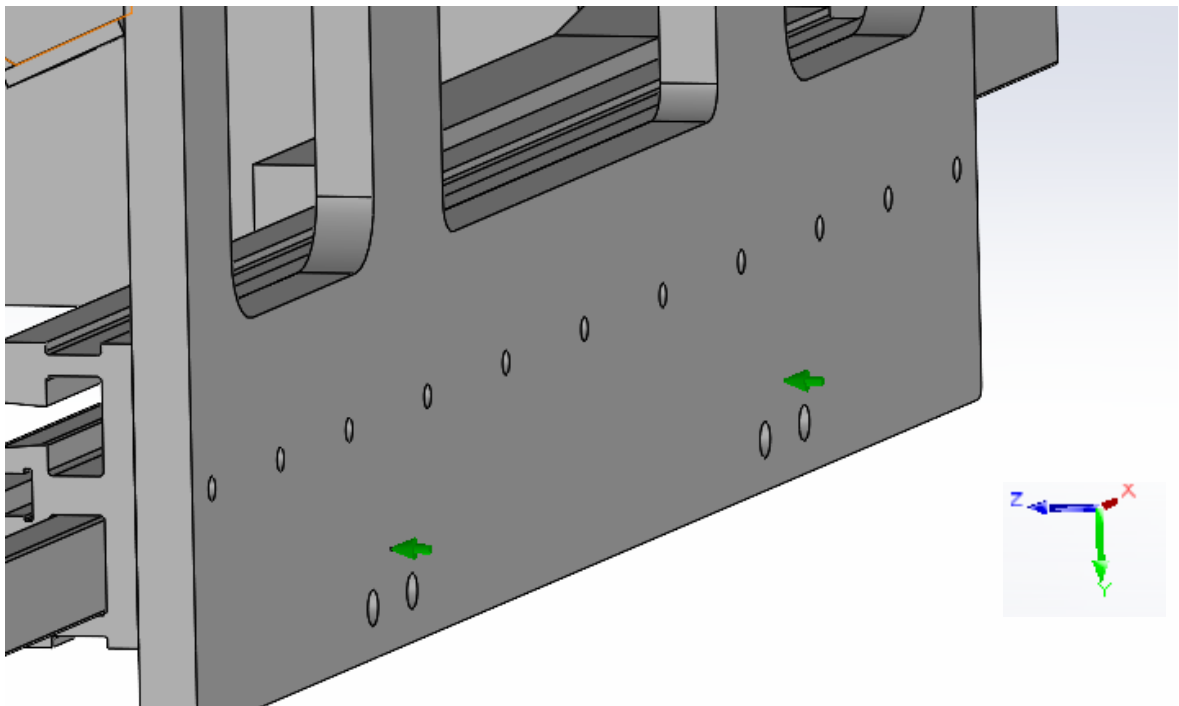


**Figure 13.** Frame plate constraints (green arrows).

The hooks that are used to fasten the frame to the carriage are constrained so that translations are prevented along the Y- and Z-axis. Also, the left hook is constrained from one corner to prevent translations along X-axis. The applied constraints are presented in figure 14.

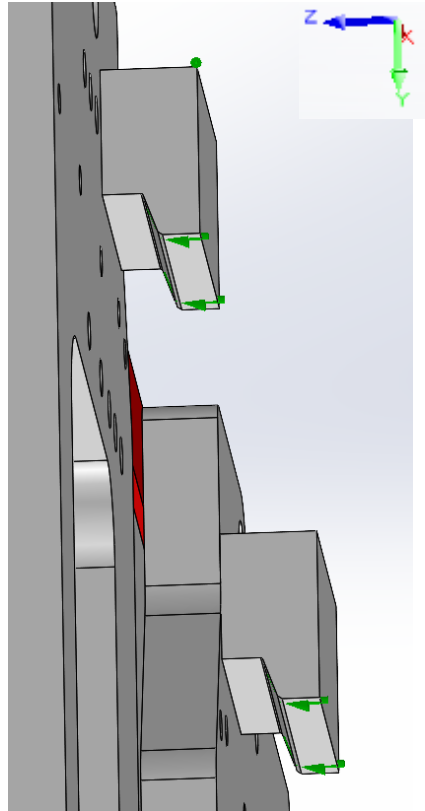


**Figure 14.** Constraints on the hooks.

All the parts of the assembly are put together using Solidworks assembly tools. And by default, Solidworks defines a bonded connection to parts that are in contact by the surface. Corresponding feature e.g. FEMAP is glued contact. Some more specific definitions are needed to make sure the analysis gives right results. There are two more different types of contact, and they are:

- Contact
- Allow penetration

In these analyses the “allow penetration” is not used. The “contact” means that the two components are not bonded but they are not allowed to penetrate each other. The contact is used between the aluminum profiles and the frame plate. It is used also for the arms and the aluminum profiles. The pallet is simulated using virtual walls. The walls are set at the area where the pallet would touch the arms. This way the model works properly. The surfaces that are with no penetration, bonded and virtual wall are shown in figure 15.

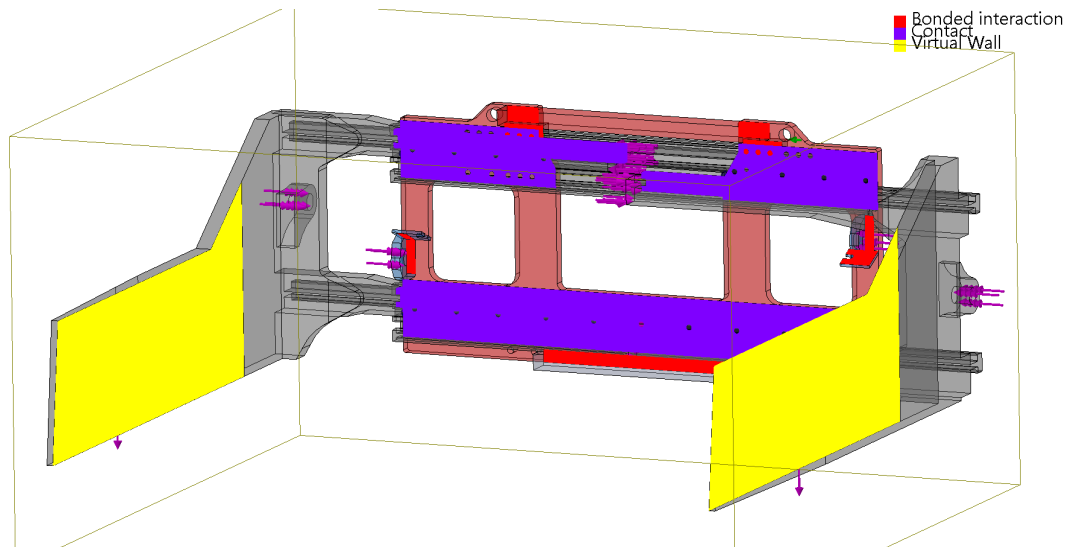


**Figure 15.** Contact visualization plot from Solidworks.

In figure 15 the purple visualizes contact, red bonded connection and yellow is a virtual wall where the pallet touches the arms. In this figure it is LC2 where  $E_P$  is 300 mm.

From the initial data provided by Auramo was given the distance of the bale edge from the arm backplate. The virtual wall differs from normal constraints that it does not constraint the nodes. Constraining the nodes would give false results from the analysis. With the walls the force transfers the right way to the profiles and from there to the frame. The walls work the same way as there would be a modelled bale between the arms.

### 2.3.3 Bolted connection

As mentioned earlier the aluminum profiles are fastened to the frame plate using M16 hex bolts. These bolts are defined using Solidworks bolted connection feature. The friction factor  $\mu$  for the bolts is 0.2 (SFS-EN 1993-1-8. 2005. p. 33). The bolt data is presented in table 3.

*Table 3. Bolt data (mod. SFS EN ISO 898-1. 2013. p. 8-10.).*

M16 Hex bolt data	
Tensile stress area,	157 mm <sup>2</sup>
Bolt strength, $R_m$	1220 MPa
Ultimate tensile load, $F_m$	192 kN

From Solidworks we get the forces acting on the bolts, but we will calculate analytically what the bolt can withstand and make sure that the bolts will not break. The calculations are done according to SFS-EN 1993-1-8. The shear strength  $F_{v,Rd}$  of one bolt is calculated as shown below (SFS-EN 1993-1-8. 2005. p. 27).

$$F_{v,Rd} = \frac{\alpha_v * f_{ub} * A_s}{\gamma_{M2}} \quad (2)$$

In equation 2  $f_{ub}$  is the bolt ultimate strength,  $A_s$  is the tensile strength area of the bolt and  $\gamma_{M2}$  is the partial safety factor for bolts.

The design tension resistance per bolt  $F_{t,Rd}$  can be calculated as shown below (SFS-EN 1993-1-8. 2005. p. 27).

$$F_{t,Rd} = \frac{k_2 * f_{ub} * A_s}{\gamma_{M2}} \quad (3)$$

The constant  $k_2$  in equation 3 is 0,9 and the constant  $\alpha_v$  in equation 2 is 0,5 (SFS-EN 1993-1-8. 2005. p. 27).

The utilization ratio will also be calculated to see how much of the bolt's capacity is used. For the calculation is needed the shear and tension forces from the bolts. This is the linear combination of both. The utilization ratio can be calculated as shown below (SFS-EN 1993-1-8. 2005. p. 27).

$$\frac{F_{v,Ed}}{F_{v,Rd}} + \frac{F_{t,Ed}}{1,4 * F_{t,Rd}} \leq 1 \quad (4)$$

In equation 4  $F_{t,Ed}$  is the design tensile force per bolt for the ultimate limit state and  $F_{v,Ed}$  is the design shear force per bolt for the ultimate limit state.  $F_{v,Ed}$  and  $F_{t,Ed}$  will be got from the analyses.

### 2.3.4 Mesh

The preliminary analyzes was done using a quite coarse mesh. The model was meshed using 4 node tetrahedron volume elements. All the four different loading cases was analyzed using the same mesh size. This was done by just copying the study four times and just applying the constraints and loads on different spots depending on the loading case. Using the same mesh size helps to compare the preliminary analyzes to each other. The mesh information is shown below in figure 16.

Study name	LC2P (-Default-)
Mesh type	Solid Mesh
Mesher Used	Curvature-based mesh
Jacobian points for High quality mesh	16 points
Mesh Control	Defined
Max Element Size	113,159 mm
Min Element Size	22,6318 mm
Mesh quality	High
Total nodes	276513
Total elements	157176
Maximum Aspect Ratio	310,88
Percentage of elements with Aspect Ratio < 3	71,2
Percentage of elements with Aspect Ratio > 10	9,72
Percentage of distorted elements	0
Number of distorted elements	0
Remesh failed parts independently	Off
Time to complete mesh(hh:mm:ss)	00:00:11
Computer name	HEF62

**Figure 16.** Mesh information on preliminary analyses.

The meshed model for the preliminary analyses is presented below in figure 17.

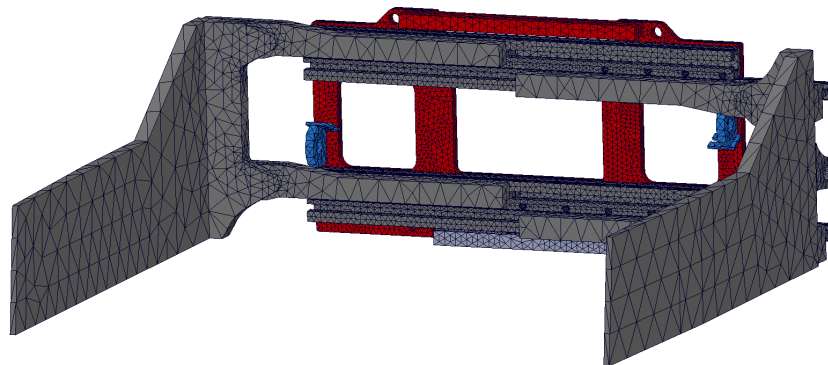


**Figure 17.** Mesh for the preliminary analyses.

The mesh was created first globally using the global meshing tool. Then mesh control is added for places that need more dense mesh. These places were:

- Bottom of the T-profile of the arms
- Opposite surface of the aluminum profile
- Frame plate
- Stiffeners of the frame plate

The reason why these places were chosen was due to the contact that need more dense mesh to work properly, and rest of the parts are probably the most critical for the structure's durability.

#### 2.4 Results from the preliminary analyses

In this chapter are presented the results of the preliminary analyzes. As said earlier all the analyzes were done using the same mesh size so that the results can be compared reliably to each other.

Below in figure 18, 19, 20 and 21 are presented the VonMises stresses of LC1, 2, 3 and 4 in the scale of 0-355 MPa.

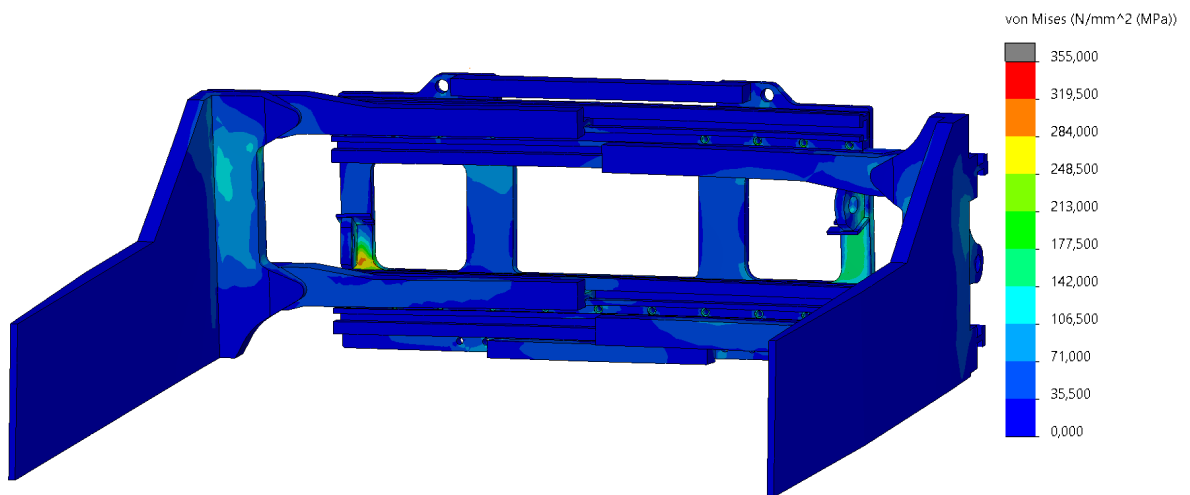


**Figure 18.** LC1 VonMises stresses.

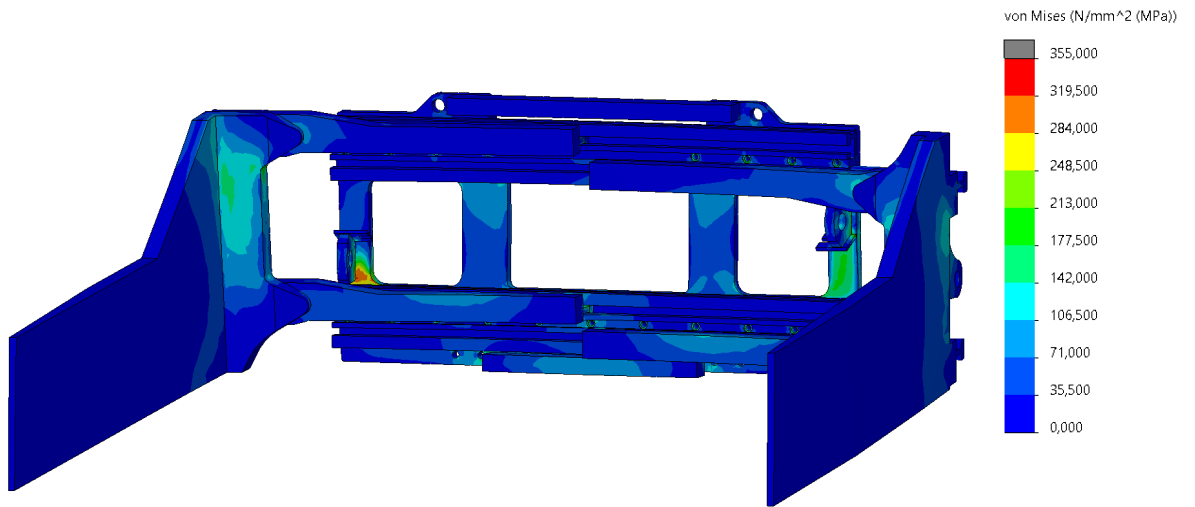


Figure 19. LC2 VonMises stresses.

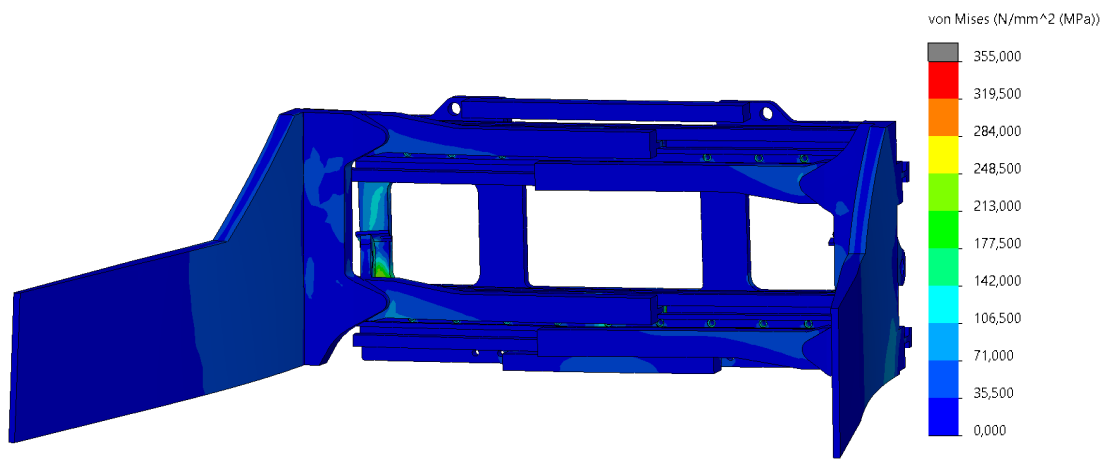


Figure 20. LC3 VonMises stresses.

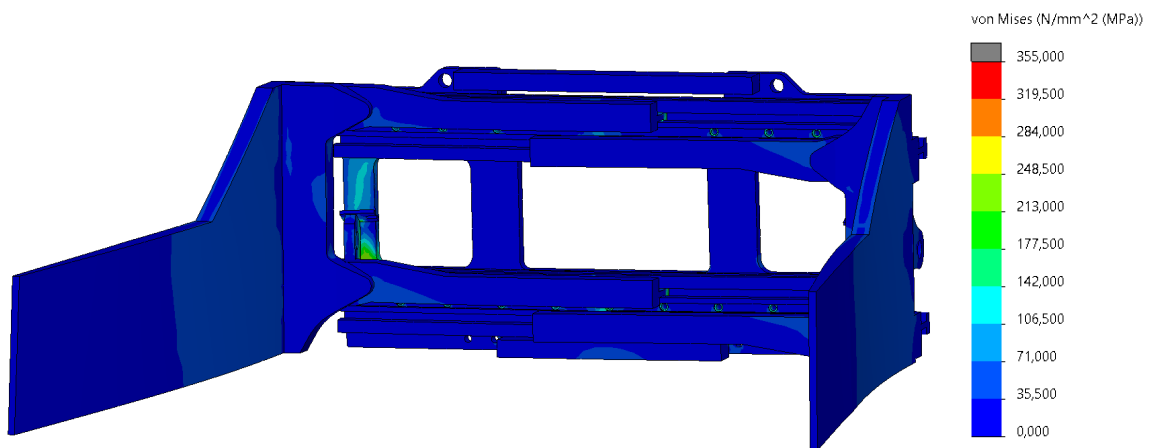
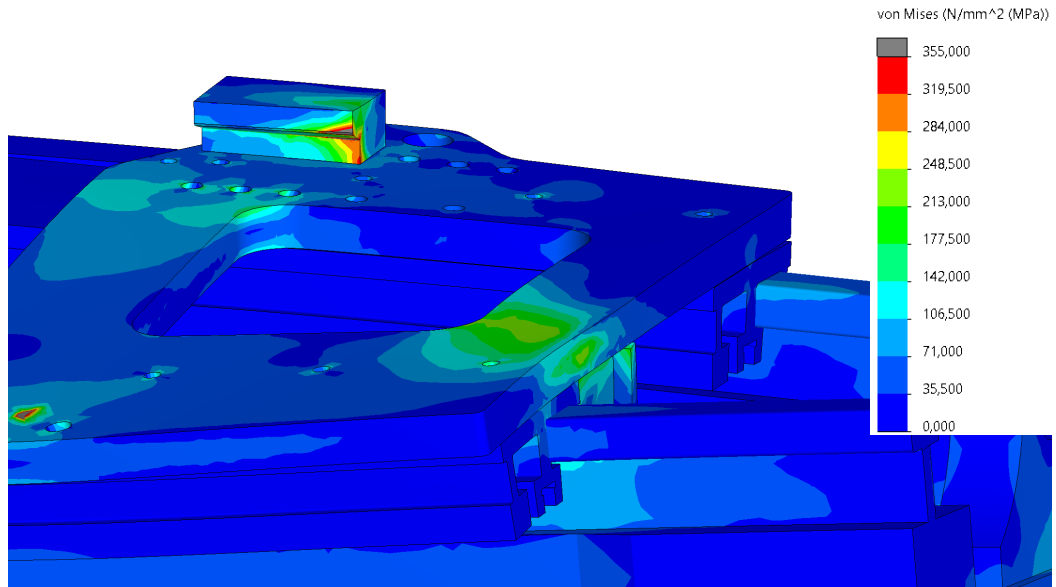


Figure 21. LC4 VonMises stresses.

The cylinder fastener bends the plate and then the arms cause also bending. The plate bends which is bad. The bending can be seen below in figure 22.



**Figure 22.** Bending at the cylinder fastener, stress scale 0-355 MPa.

There are some stress peaks in the bale clamp caused by the constraints, but they are singularities that can be ignored. The stresses measured from the same point are presented below in table 4 and the point measured from in figure 23.

*Table 4. Maximum stresses at the cylinder bracket.*

Loading case	VonMises stress [MPa]
LC 1	297
LC 2	316
LC 3	237
LC 4	230

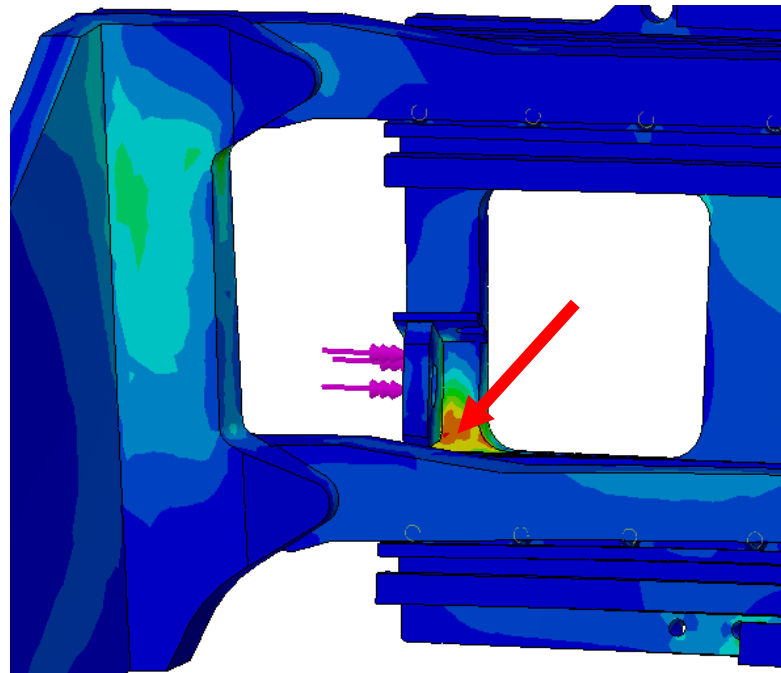


**Figure 23.** Point where the stresses are measured from.

The stresses in the aluminum profiles are quite minimal and the stresses are at maximum 70 MPa. Most of the stresses are caused by the bending that occurs from the clamping of the bale.

Below in figure 24-31 are presented the displacements of all the loading cases. The displacements are scaled 20 times to see them clearly.

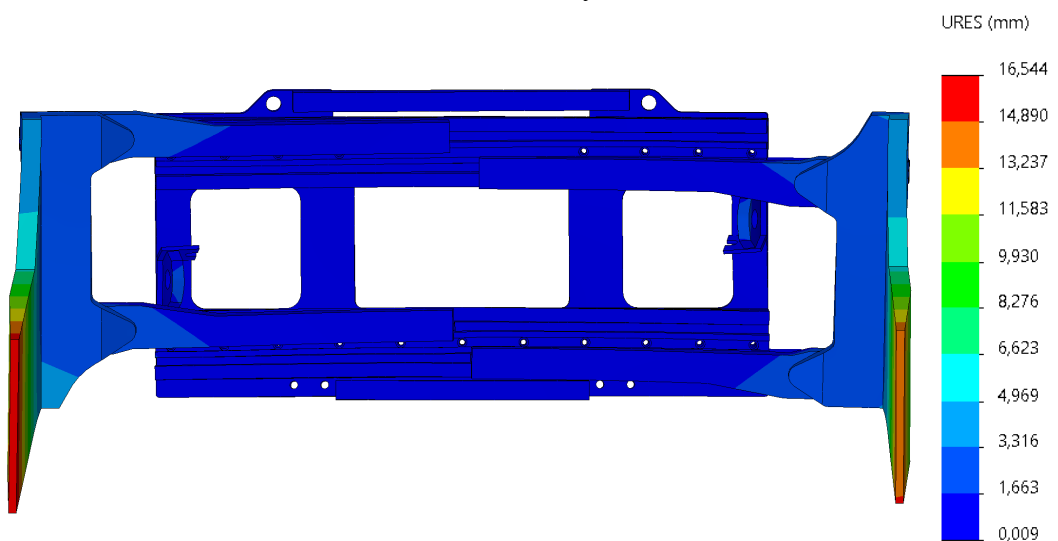


**Figure 24.** LC1 displacements from front, scaled 20 times.

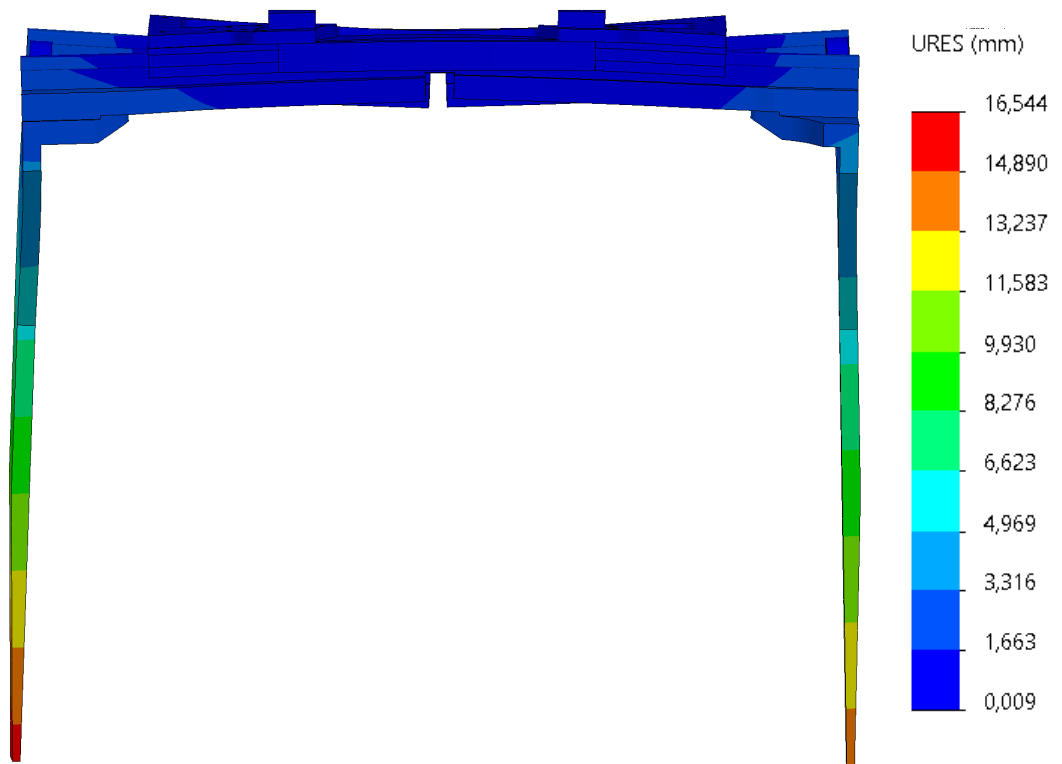


**Figure 25.** LC1 displacements from top, scaled 20 times.

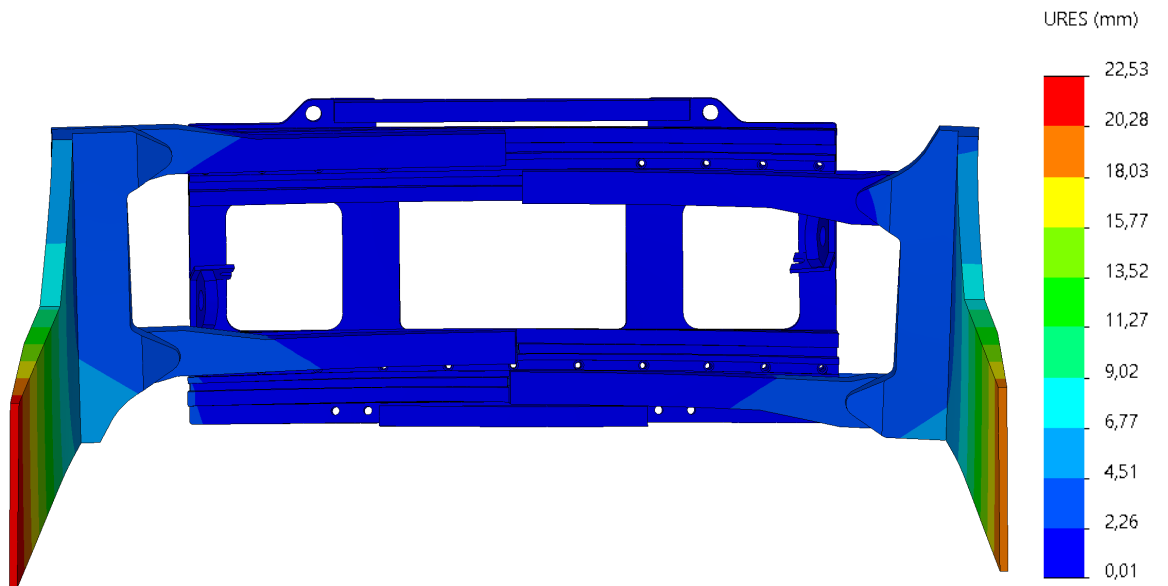


**Figure 26.** LC2 displacements from front, scaled 20 times.

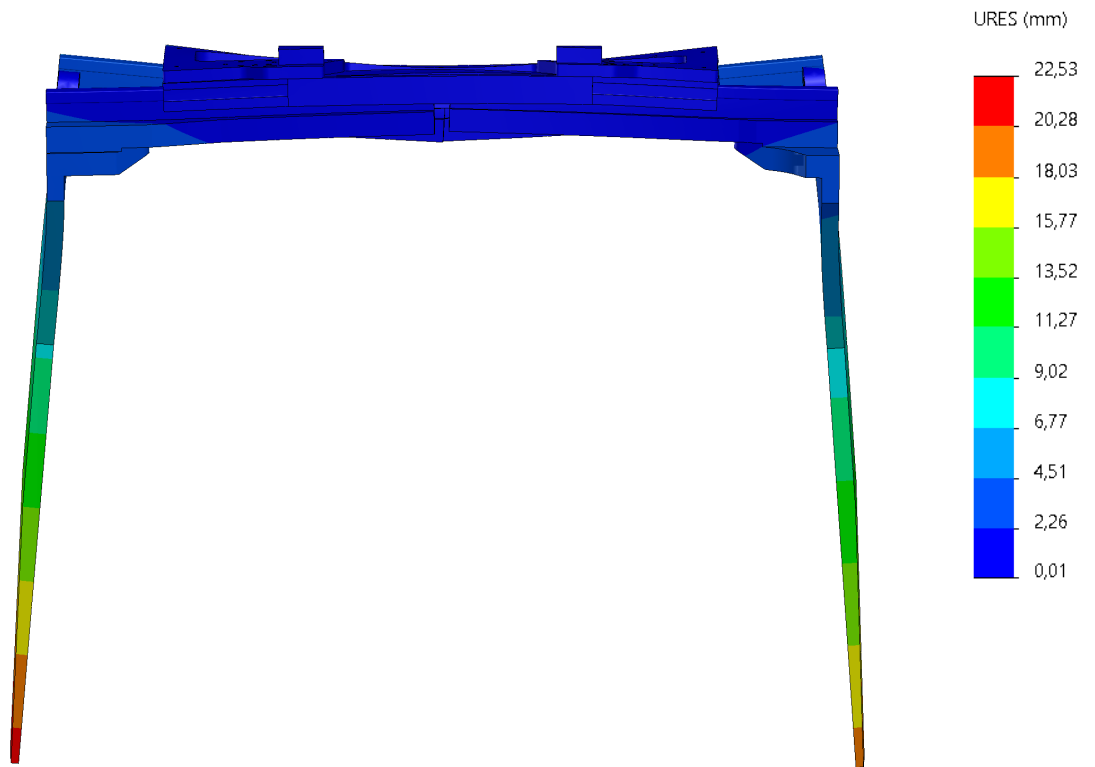


Figure 27. LC2 displacements from top, scaled 20 times.

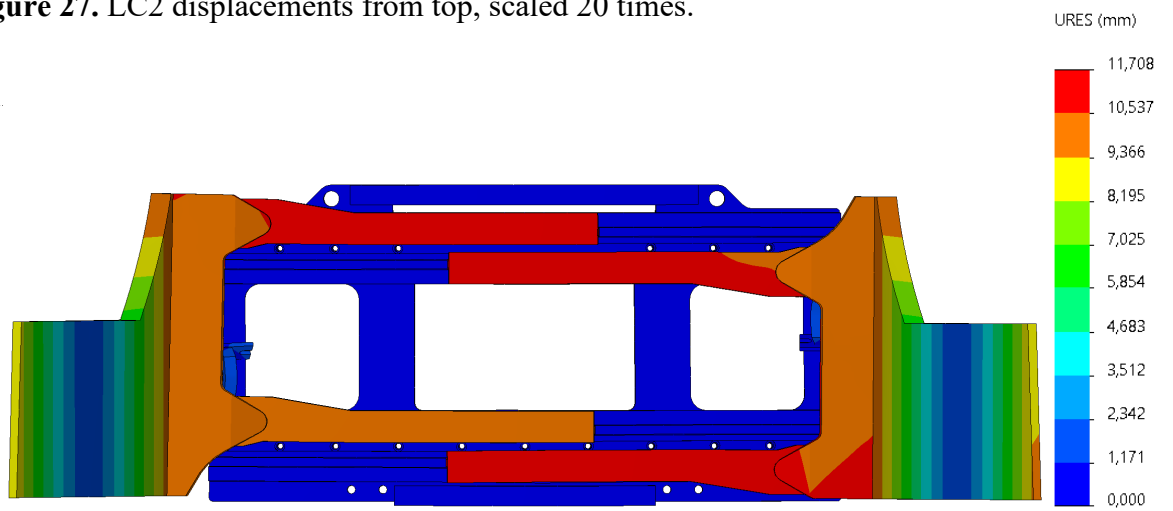
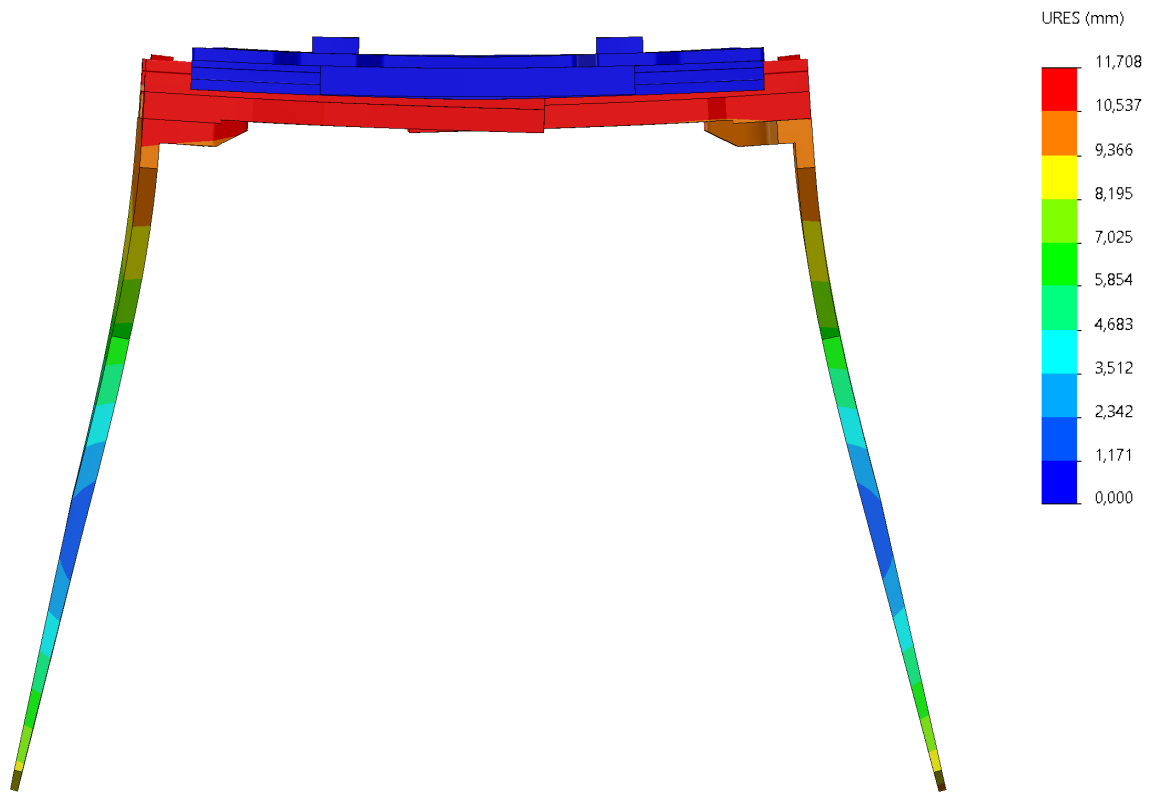
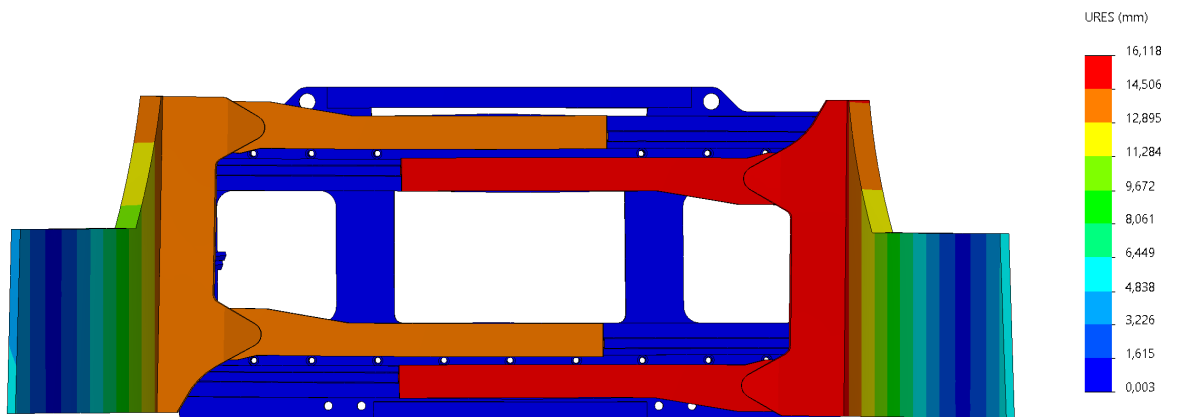


Figure 28. LC3 displacements from front, scaled 20 times.



**Figure 29.** LC3 displacements from top, scaled 20 times.



**Figure 30.** LC4 displacements from front, scaled 20 times.

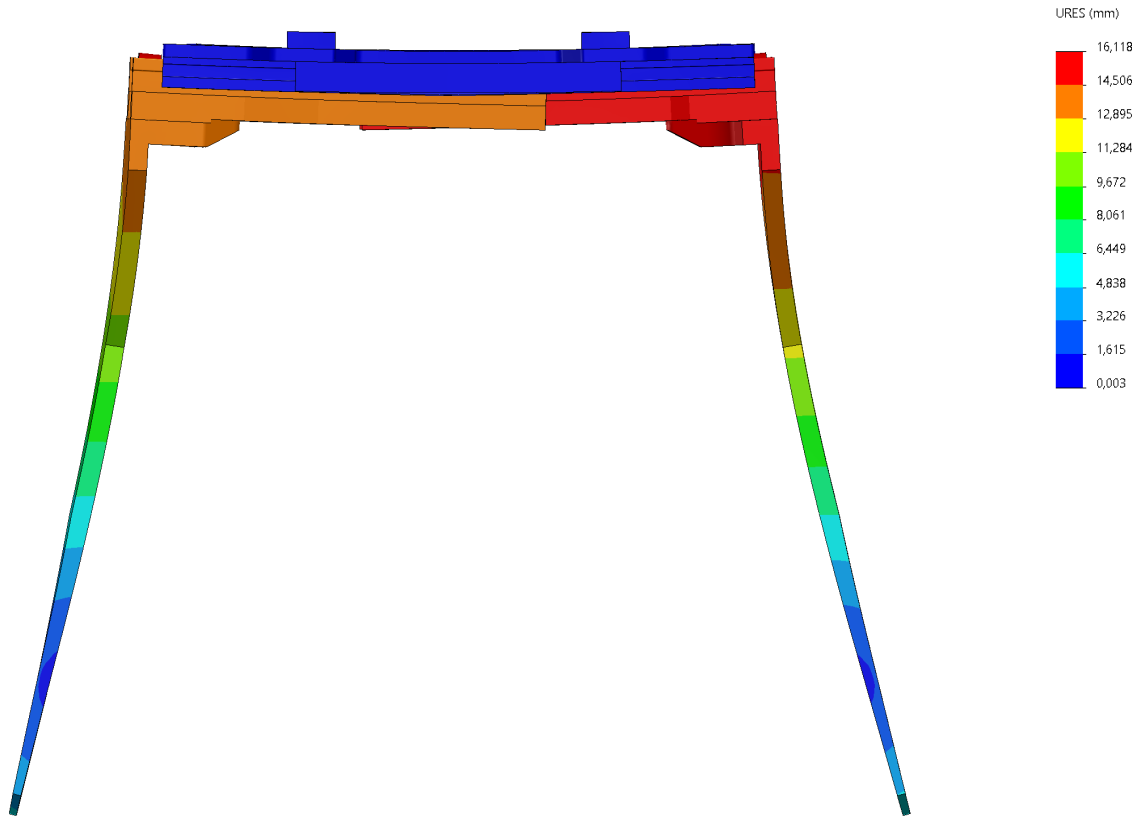


**Figure 31.** LC4 displacements from top, scaled 20 times.

The maximum displacements in each loading case are presented below in table 5.

*Table 5. Maximum displacements in each loading case.*

Loading case	Maximum displacement [mm]	Frame plate maximum displacement
LC1	16,5	1,5
LC2	22,5	2,4
LC3	12	0,8
LC4	15,4	0,7

From the displacements we can see that the biggest one is in loading case 2 where  $E_p = 300$  mm. As seen from the pictures the further the bale is from the arm back plates the less the frame plate bends. The further the bale is the more the arms can move inwards along the aluminum profiles. When the bale is closer to the plates it causes the plate to bend more and causing larger displacements and then also bigger stresses.

### 2.4.1 Bolt forces

The bolted connection between the frame plate and aluminum profile results are presented in this chapter. From Solidworks are taken the bolt forces in each bolt. The bolt forces are listed in appendix I. The pretension force caused by the tightening torque in every bolt is 45 573 N. This was calculated using the FE-model but without any clamping or other loads. There is not added friction between the aluminum profiles and the frame plate. From the results can be seen that the bolts are not the limiting factor in the bale clamp structure. The bolted connection and forces will be investigated more precisely in the final analyzes to confirm the results. The design shear and tension forces for each bolt are calculated below in table 6.

Table 6. Design tension and shear forces per bolt.

Type	Force [N]
Shear $F_{v,Rd}$	76 616
Axial $F_{t,Rd}$	137 909

The strength class of the bolts is 12.9 so the ultimate tensile strength  $R_m$  is 1220 MPa and not a single bolt is near those kinds of stresses. The axial and shear forces are listed in appendix I. The forces are the combination of the pretension force and the force caused by the loads. A bolt graph based on bolt number 14 is presented below in figure 32.

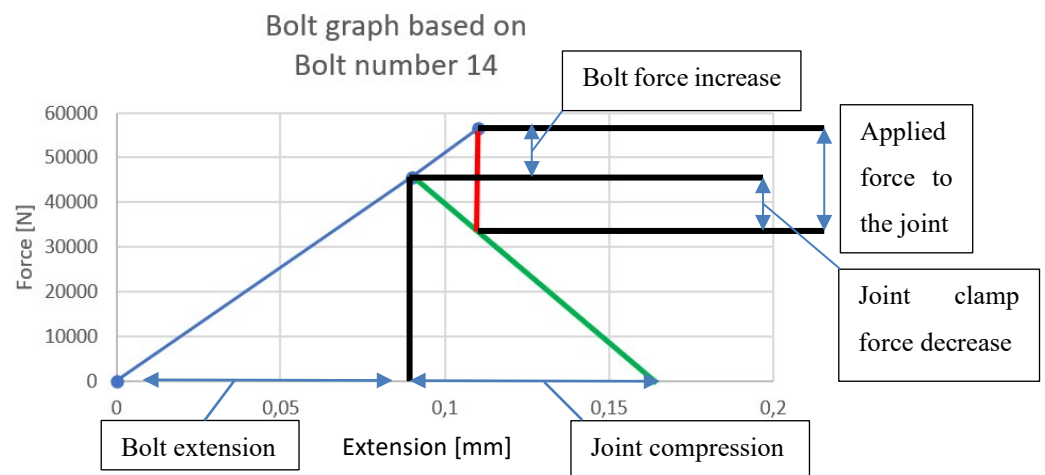
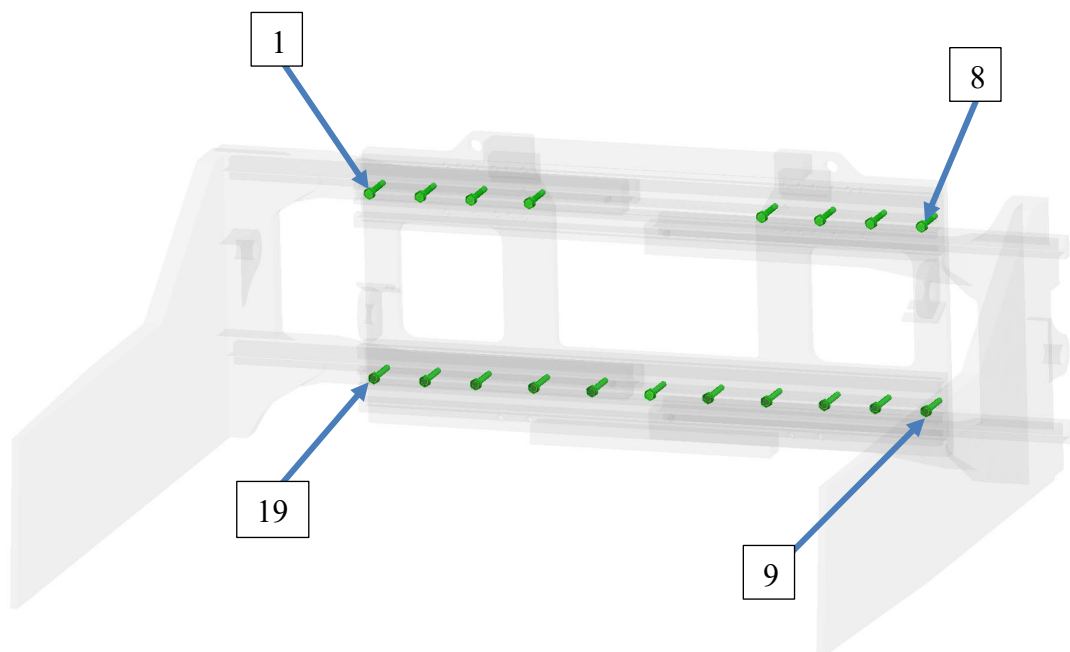


Figure 32. Bolt graph of bolt number 14.

In appendix I is also listed the utilization ratio and factor of safety. The factory of safety and the utilization ratio of each bolt is also listed. The utilization rate of every bolt was at minimum 24 % and at maximum 34 %. This gives that the factory of safety for static load is around 4 on every bolt. The bolts are numbered in appendix I that number one is the top left one and then the numbering goes from left to right at the top. Then the numbering starts from number nine at the bottom right and goes from right to left. The numbering is presented below in figure 33.



**Figure 33.** Bolt numbering.

The aluminum profile and the frame plate are allowed to slide on top of each other. The contact between the aluminum profile and the frame plate detaches from the corners. This is not critical if it doesn't detach by the bolts because then the stress variation would be so big that the fatigue life for the bolts would be minimal. The part where the aluminum profile comes off the frame plate is presented below in figure 34.

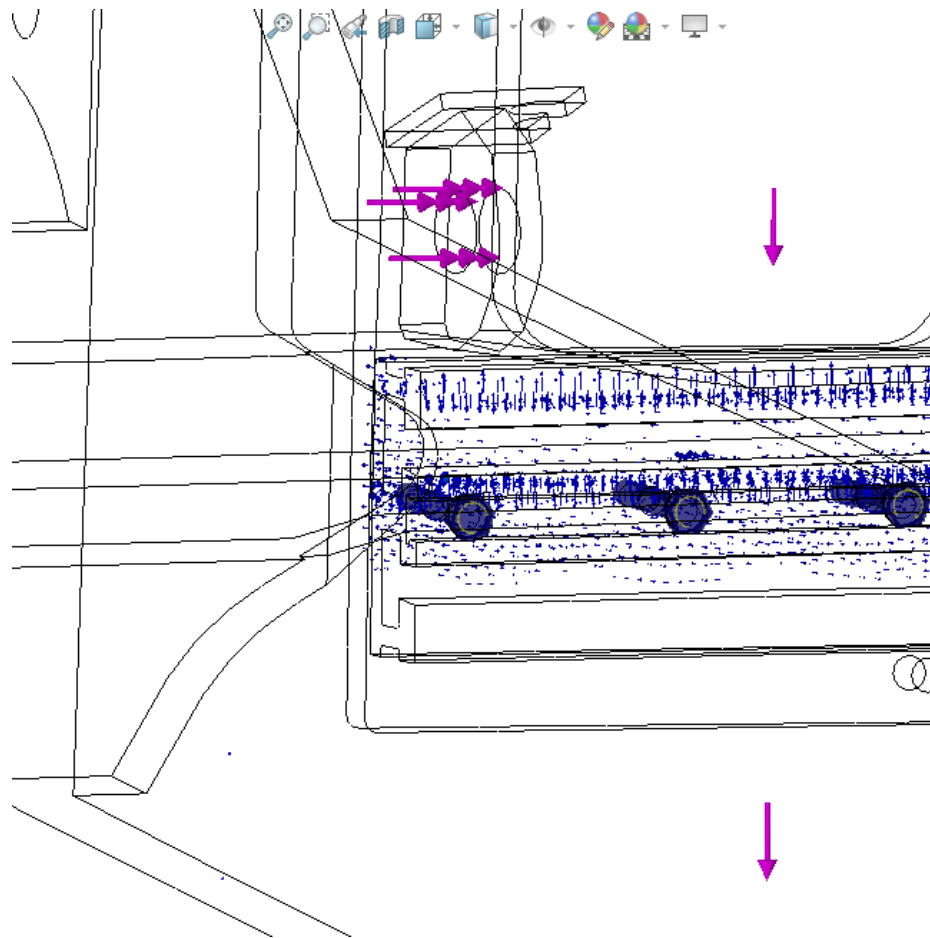


**Figure 34.** Spot where the aluminum profile and frame plate contact detaches.

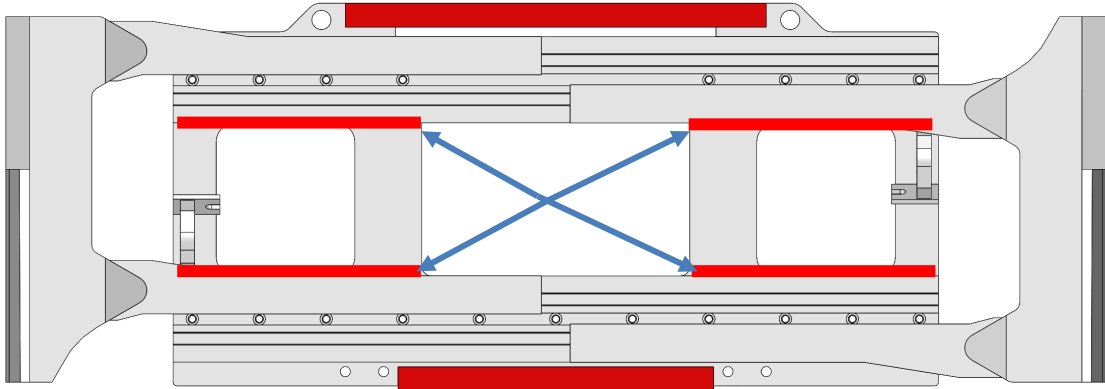
The blue arrows shows where a contact pressure is remained. The loading case analyzed is LC2. The profile comes off from the same spot in every loading cases.

Another part that is critical for the bolted connections durability is the aluminum profile the bolt goes through. The web is quite narrow in the aluminum profile but the stresses there are at maximum around 60 MPa so this is here not the limiting factor for increasing the capacity. The fatigue of the bolts will be investigated later.

### 3 IMPROVEMENTS FOR THE STRUCTURE

In this chapter is presented the proposed improvements for the structure. The improvements are based on the point where the highest stresses occurred and how they can be reduced. The most critical point is where the cylinder is attached. The bigger peaks are on the left side since the bale clamp is not totally symmetric.

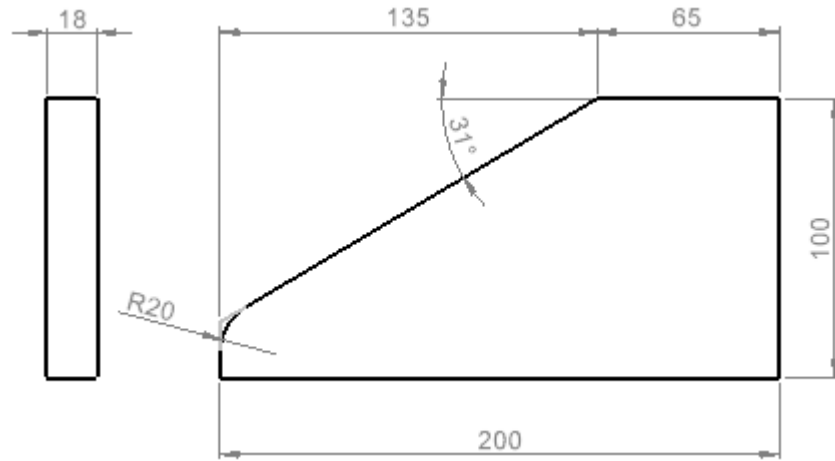
The structure must be stiffened from these points with plates. The plates will be welded to the cylinder bracket and the frame plate. This way the plate constrains the bending of the cylinder bracket so that it does not cause large forces and bending on the plate. The plates cannot be installed directly because there is no extra room between the bracket and the aluminum profile. This means the plate must be modified so that the stiffeners can be welded. The height of the plate must be changed so that material will be added between the brackets and the cut outs. The place where the material will be added is presented with red lines shown with arrows in figure 35.



**Figure 35.** Modification of frame plate.

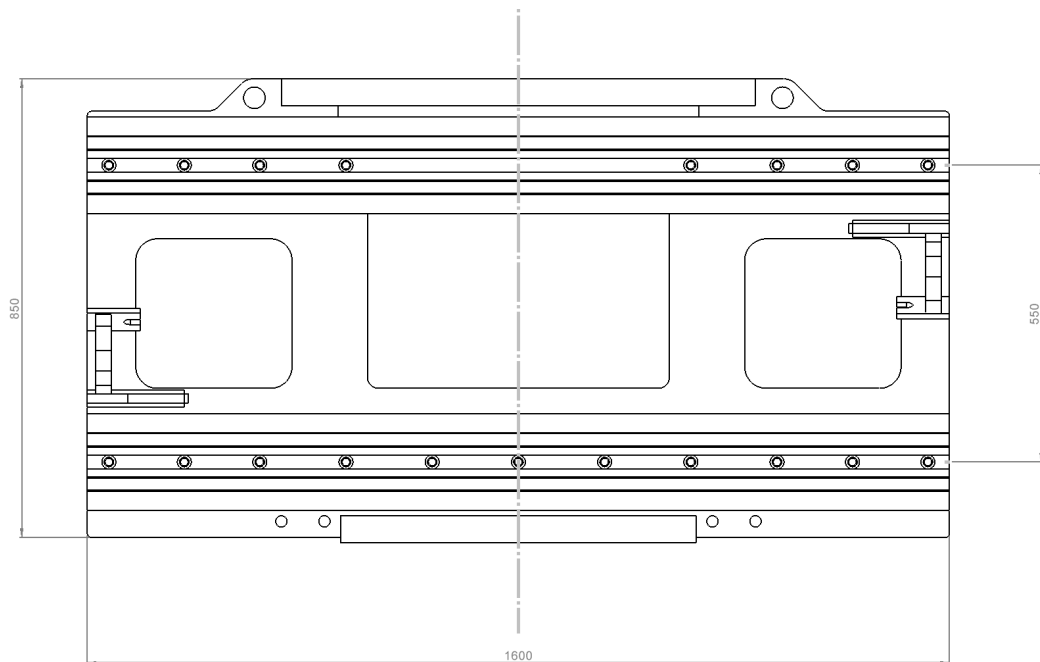
The amount of material added is 25 mm per side so total added is 50 mm. The height changes then by 50 mm and the stiffeners fits this way. The Structure will be a little bit heavier because the cut outs stay the same size. The lighter the structure the better but this is the only way the stiffeners fit. When the frame plate is modified then the distance of the aluminum profiles changes also, and this means the arms need to be modified so that they fit to the new

plate. The stiffeners are made from S355 like the frame plate. The thickness is 18 mm. The dimensions of the plate are presented below in figure 36.



**Figure 36.** Stiffener plate dimensions.

The biggest need of the stiffening is by the cylinder bracket so the stiffener can be narrowed down when going further away from the bracket. This way there is no extra material, it also looks a lot better and takes as little space as possible. The new dimensions of the frame plate are presented below in figure 37.



**Figure 37.** Modified frame plate dimensions [mm].

All the holes remain the same, but they are just moved 25 mm up/down from the centerline. The cylinder bracket's location remains the same (vertical distance between them). The stiffeners will be welded with a a5 fillet weld. It is not needed a bigger weld because the weld is influenced only by a shear force caused from the bending. The Stiffeners are also welded to the cylinder bracket to give even more stiffness. The cylinder brackets are welded with a a10 fillet weld to the frame plate and these welds are added to the model for the fatigue calculations. Also, for welding the bracket from the top to the stiffener some minimal adjustments for the bracket geometry are done. This way a bevel-groove weld can be done. The improved bale clamp model is presented below in figure 38.

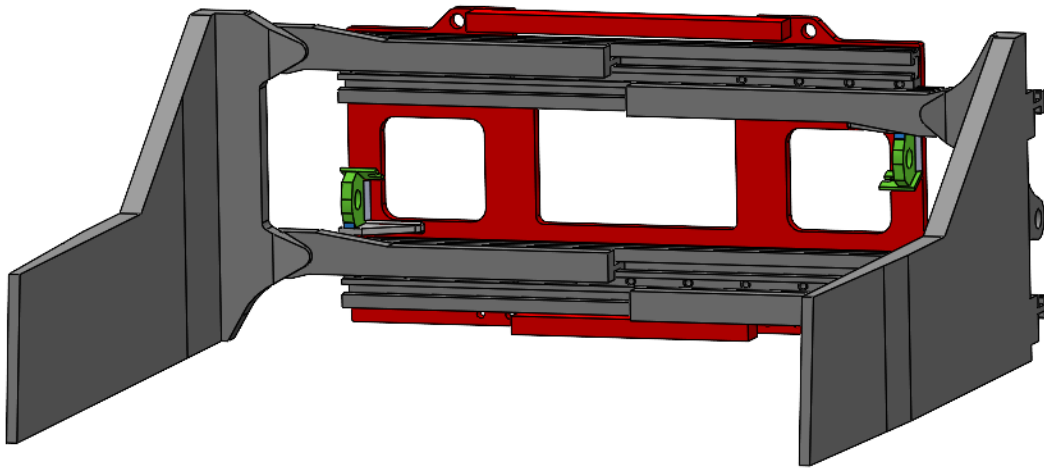


**Figure 38.** Improved bale clamp model.

## 4 FINAL ANALYSES

In this chapter is presented the analyzes on the improved structure. The chosen loading cases are based on the preliminary analyzes and information provided by Auramo. The chosen loading cases are LC2 and 3. LC2 was chosen because it was the most critical loading case based on the stresses in the structure. LC3 was chosen because it is the loading case which is more critical of the cases where only clamping is done and no lifting. The changes made from the preliminary analyzes focus on making the mesh finer and adding the stiffeners. The a5 fillet weld is also modelled into the model to get more precise results from the analyzes.

### 4.1 Mesh

The mesh is needed to be denser in certain spots where the highest stresses occur and where there is contact between two components. The mesh is made more denser for these parts:

- Frame plate
- Stiffener plates
- Weld at stiffeners
- Surfaces at bottom of T-profile
- Surfaces in aluminum profile where the T-profile touches
- Welds

The mesh size for each part with denser mesh is presented below in table 7.

*Table 7. Mesh sizes.*

Part	Element size [mm]
Frame plate	9
T-profile	14
Weld	2,5
Stiffeners	7
Aluminum profiles	20
Cylinder bracket	5
Welds	2.5

The mesh size was kept the same in both LC2 and 3 to keep the results easily comparable. The overall mesh data is presented below in figure 39.

Study name	Static 4 from [LC2P] (-Default-)
Mesh type	Solid Mesh
Mesher Used	Standard mesh
Automatic Transition	Off
Include Mesh Auto Loops	Off
Jacobian points for High quality mesh	16 points
Mesh Control	Defined
Element size	62,2256 mm
Tolerance	0,15 mm
Mesh quality	High
Total nodes	749993
Total elements	472565
Maximum Aspect Ratio	55,893
Percentage of elements with Aspect Ratio < 3	93
Percentage of elements with Aspect Ratio > 10	0,945
Percentage of distorted elements	0
Number of distorted elements	0
Remesh failed parts independently	Off
Time to complete mesh(hh:mm:ss)	00:00:46
Computer name	HEF62

**Figure 39.** Mesh information for final analyzes.

#### 4.2 Constraints

The constraints will be the same as in the preliminary analyzes for the specific loading cases. The only difference is in the component interactions. The stiffeners will be with contact against the frame plate and will be bonded using the a5 fillet welds. This gives the most realistic results. The same case is with the cylinder brackets if they would be also bonded. If the stiffeners would be bonded from the whole bottom surface to the plate the results would overestimate the stiffness and strength. Because it would correspond flat-strength weld and that would be an unnecessary big weld. A friction coefficient of 0.1 was also added between the aluminum profile and the frame plate. The friction coefficient is bigger than 0.1 but this is on the safe side when looking at the bolted connections. The bigger the friction, the less there will be risk for the faces of the aluminum profile and the frame plate to slide. This is because the friction has a big role in the bolted connection. The exact constant depends on the material surface quality. The component interactions are presented below in figure 40. The virtual wall is for loading case 2 where  $E_P = 300$  mm.

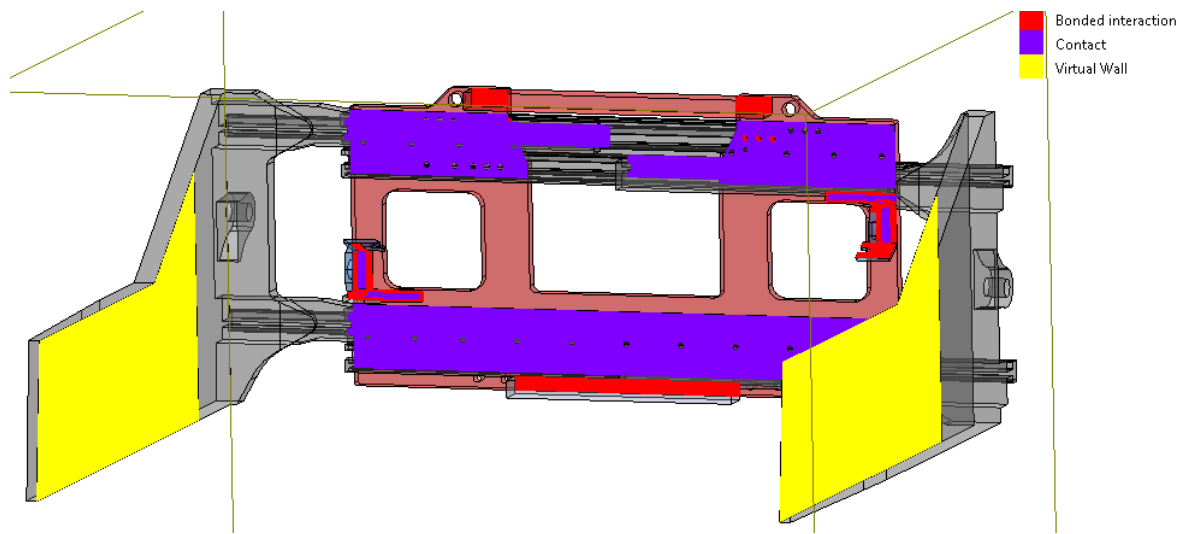


**Figure 40.** Component interaction in modified structure.

#### 4.3 Fatigue life calculations

For the final analyzes fatigue life estimations are calculated for the bolts and for the frame plate. The used loading case for fatigue calculations is LC2 obtains the largest stress ranges.

The loading cycle consists of four phases:

1. Clamping the bale
2. Lifting the bale
3. Lowering the bale
4. Releasing the bale

For the fatigue calculations one more analysis is needed. It is the same as LC2 regarding the FE-model, but the only difference is that the vertical load of the bale is not added. So only the clamping is analyzed. By adding this analysis, we get the stress range for the fatigue estimation calculations. The calculations for the bolts are done using the data from the analyzes. The fatigue analyzes for the frame plate are done using the Hot Spot method. The equations and methods are presented in this chapter 4.3.1 and 4.3.2.

##### 4.3.1 Hot Spot method

The Hot Spot method suits in this case best for estimating the fatigue life for the frame plate. This is because the frame plates most critical spot is by the cylinder bracket and by the fillet welds which the bracket is fastened to the frame plate.

Hot Spot stress is a structural stress which occurs in plate structures. It consists of a membrane and bending stress. (Niemi, E. & Kemppi, J. 1993, s. 234.) The Hot Spot -method was born when round structural tube joints were investigated in offshore-structures. (Niemi, E. & Kemppi, J. 1993, s. 251.) The structural components in the notch stress are presented below in figure 41.

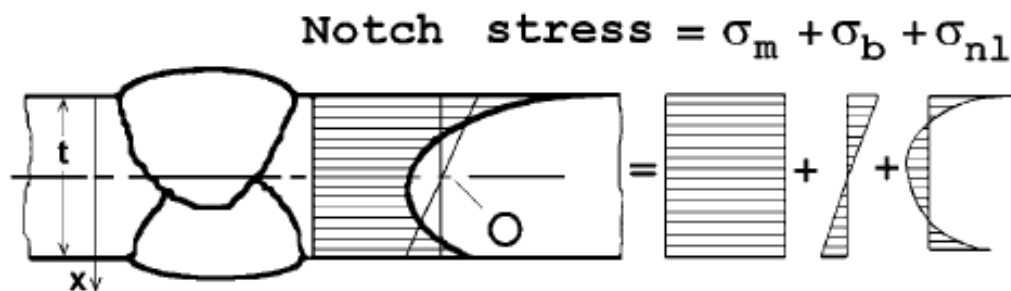


**Figure 41.** Welded joints stress components. In the equation  $\sigma_m$  membrane stress,  $\sigma_b$  bending stress ja  $\sigma_{nl}$  notch stress nonlinear part. (Hobbacher 2014, p. 14.)

The Hot Spot method fits better than the nominal stress method if the nominal stress is not acquired from the structure because of the complex geometry. If the joints misalignment is bigger than the allowed ones in the nominal stress method, then the Hot Spot method is also used. (Jonsson et al., 2016 s. 15)

The structural stress can be acquired by calculating the stress components separately. This means that we define the membrane, bending stress and the nonlinear part and then calculating together the membrane and the bending stresses. The nonlinear part is not taken to account when calculating the structural stress.

The stress distribution can be acquired using FE-analysis. Using the stress distribution, we can calculate the membrane stress  $\sigma_m$  as follows (Hobbacher 2014, p. 15.):

$$\sigma_m = \frac{1}{t} \int_{x=0}^{x=t} \sigma(x) dx \quad (5)$$

In equation 5  $\sigma(x)$  is the stress distribution through the plate thickness ja  $t$  is the thickness of the plate. The bending stress on top of the plate can be calculated as follows (Hobbacher 2014, p. 15.):

$$\sigma_b = \frac{6}{t^2} \int_{x=0}^{x=t} (\sigma(x) - \sigma_m) \left( \frac{t}{2} - x \right) dx \quad (6)$$

In equation 6  $\sigma_m$  is membrane stress which is acquired from equation 5. When the stress components are calculated the structural stress can be calculated as follows (Ruukki 2010 p. 429):

$$\sigma_{hs} = \sigma_m + \sigma_b \quad (7)$$

The notch stress nonlinear part  $\sigma_{nl}$  can also be acquired as follows (Hobbacher 2014, p. 15.):

$$\sigma_{nl}(x) = \sigma(x) - \sigma_m - \left( 1 - \frac{2x}{t} \right) \sigma_b \quad (8)$$

In equation 8  $\sigma_m$  is the membrane stress which is acquired from equation 5 and  $\sigma_b$  is the bending stress which is acquired from equation. Even though the nonlinear part is not needed when the structural stress is calculated it is still good to recognize it. It illustrates the notch effect due to weld geometry, loading of the weld, and boundary conditions of the joint, locally. When calculating structural stresses normal stresses are used.

The Hot Spot stress is calculated from two different spots, and they are:

- Weld toe at the cylinder bracket
- Weld toe at the frame plate

The point from where the normal stresses are picked through the thickness of the plate is presented with a red cross below in figure 42.

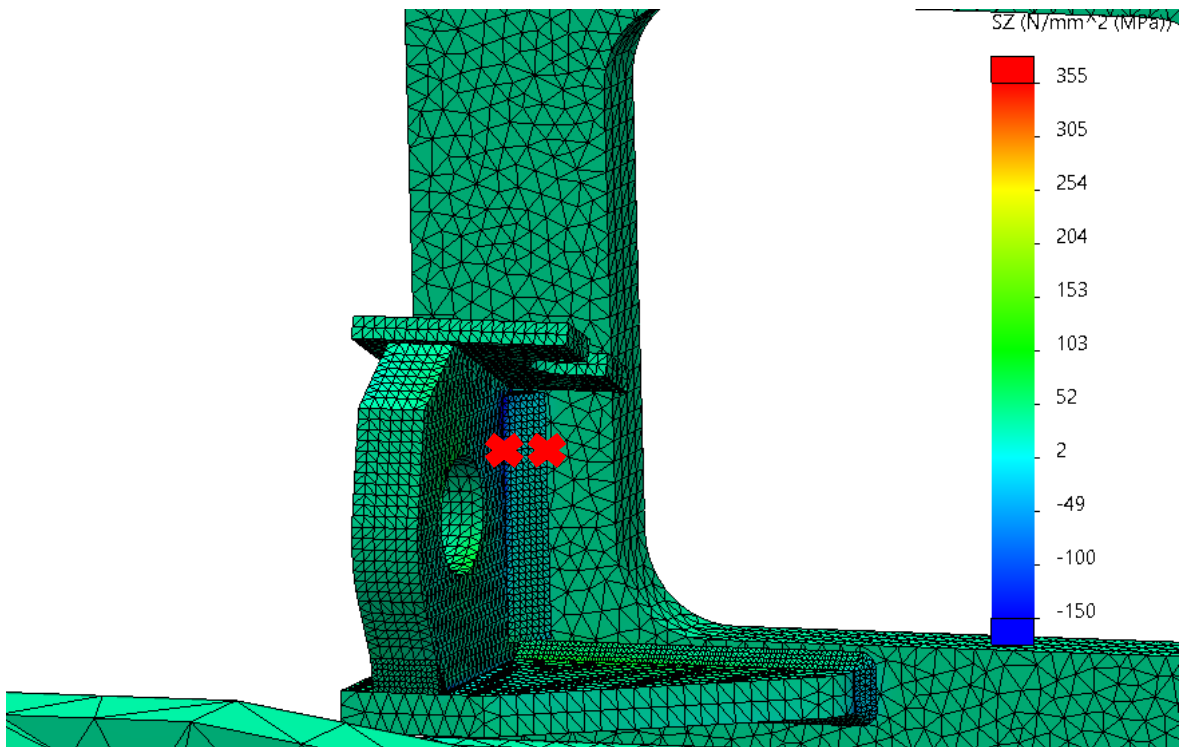


**Figure 42.** Point from where the normal stresses are picked through the thickness of the plate, marked with red crosses.

#### 4.3.2 Calculating the fatigue life

When the stress values are got from the FE-model, fatigue life can be estimated for the bolts and the frame plate. Fatigue life means how many load cycles the structure can sustain. It can be calculated as follows (Hobbacher 2014, p. 111.):

$$N_D = \left( \frac{FAT}{\Delta\sigma_D} \right)^m \cdot 2 \cdot 10^6 \quad (9)$$

In equation 9  $N_D$  is the calculated number of life cycles,  $FAT$  design value of fatigue resistance,  $\Delta\sigma_D$  design value of equivalent stress range and  $m$  SN-curve slope.

The slope  $m$  is according to IIW for low cycle fatigue 3,0 all the way to  $N = 10^7$  and for high cycle fatigue 5,0 all the way to  $N = 10^8$ . So, for equation 9 a suitable  $m$  coefficient and  $FAT$ -class for the situation and then we can calculate the estimated fatigue life. (Hobbacher 2014, p. 41.) The  $FAT$ -class is determined by the type of geometry the joint has that is analyzed when using the structural stress. In this case  $FAT = 80$  MPa is used for the calculations. For the bolt  $FAT = 50$  MPa is used (SFS-EN 1993-1-9. 2008. p. 20).

#### 4.4 Results from final analyzes

In this chapter the results are presented from the analyses made of the improved structure. The presented loading cases are 2 and 3. The results are presented of the static situations and the fatigue life calculations for LC2.

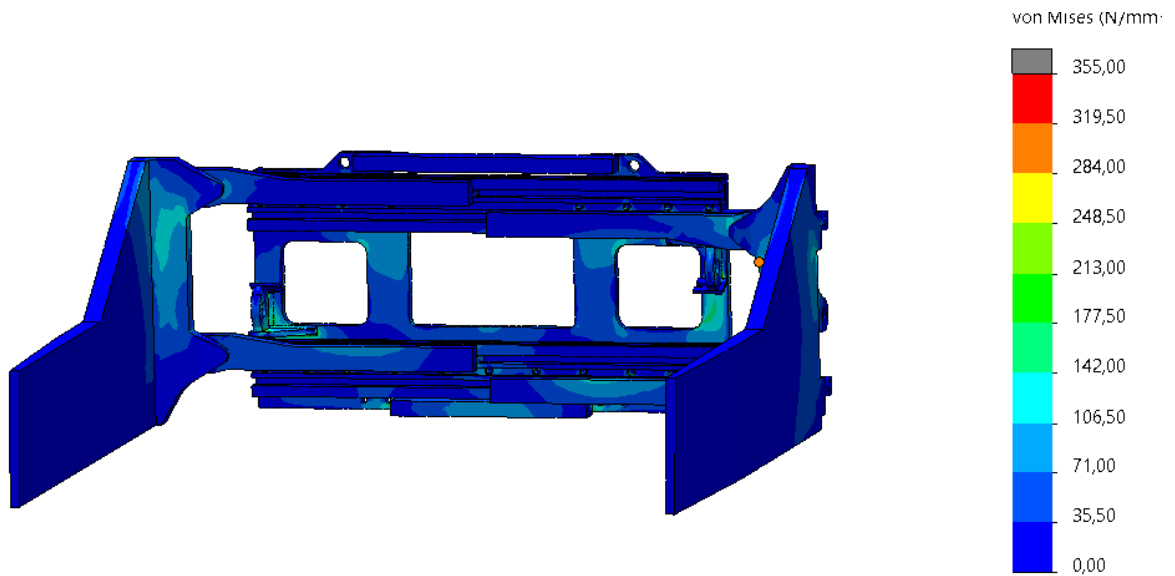


**Figure 43.** LC2 VonMises stresses.

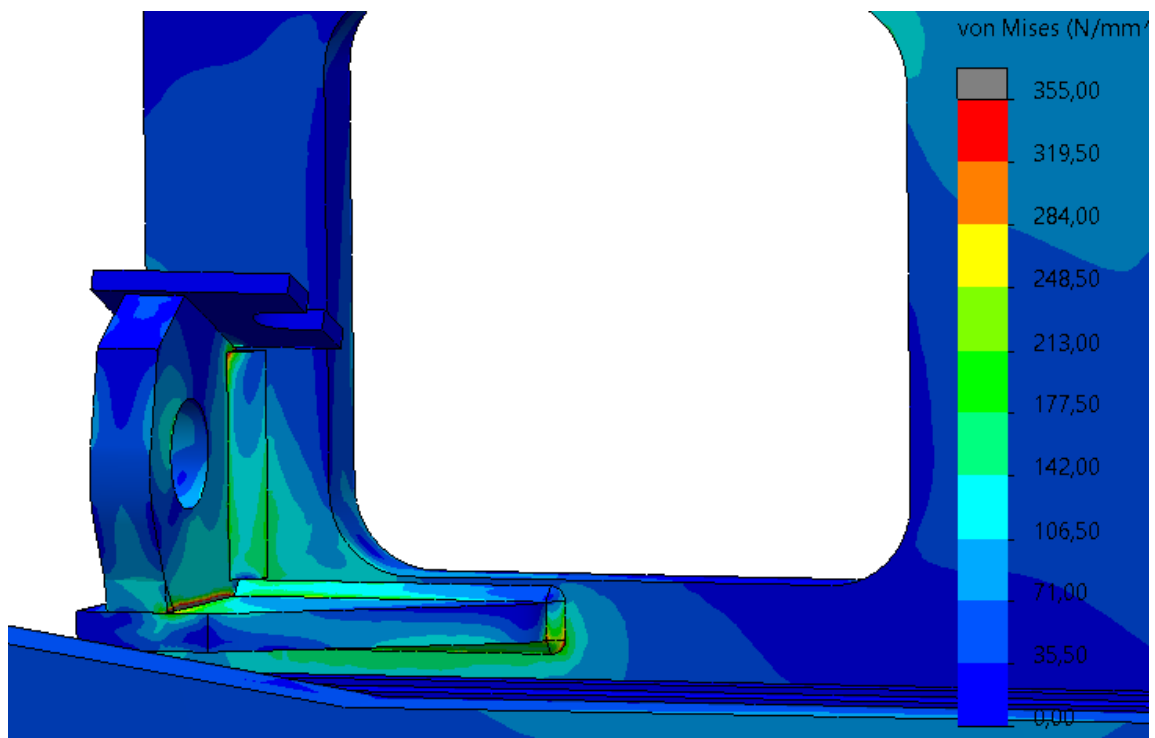


**Figure 44.** LC2 VonMises stresses at cylinder bracket.

There is a reduction of the bending after adding the stiffeners by the cylinder brackets. This can be seen in figure 45.

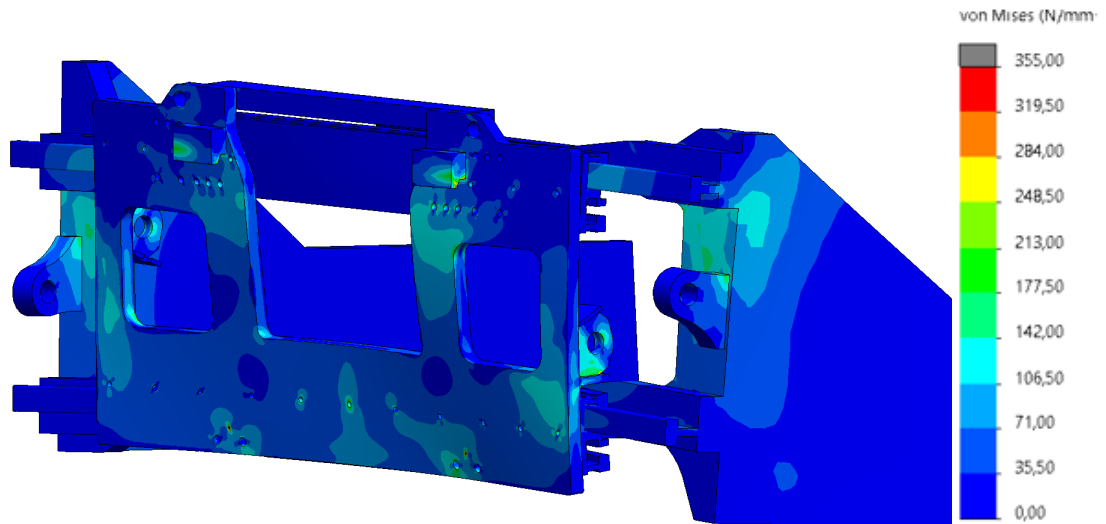


**Figure 45.** LC2 plate deformation from back, displacements scaled 11 times.

The stresses in loading case 3 are minimal as seen below in figure 46 and 47. The biggest peaks are still at the bracket, but they are also at around maximum of 140 MPa. The stress on the weld is also minimal.

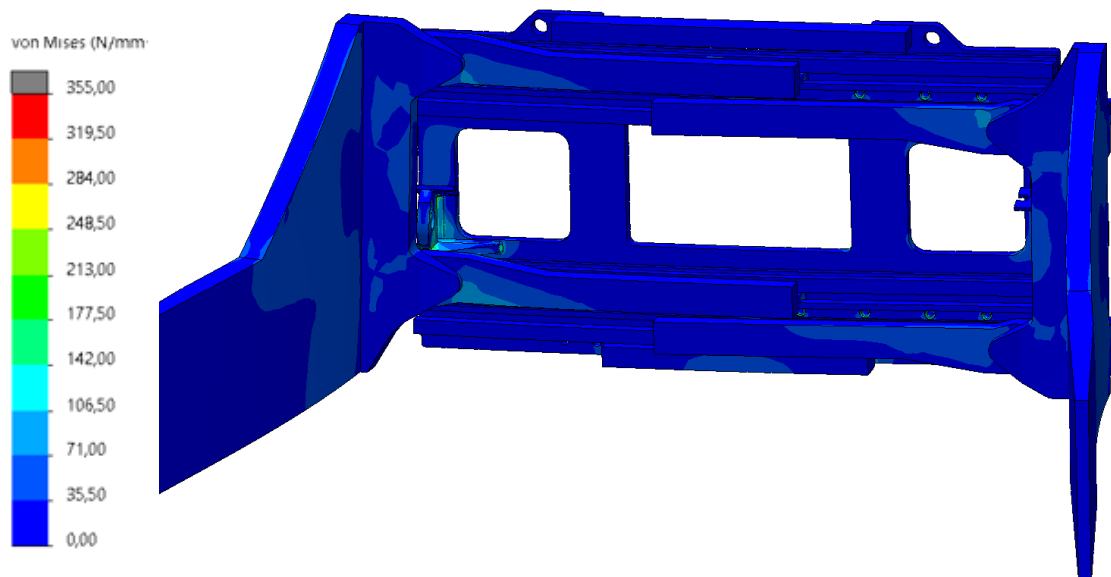


**Figure 46.** LC3 VonMises stresses.

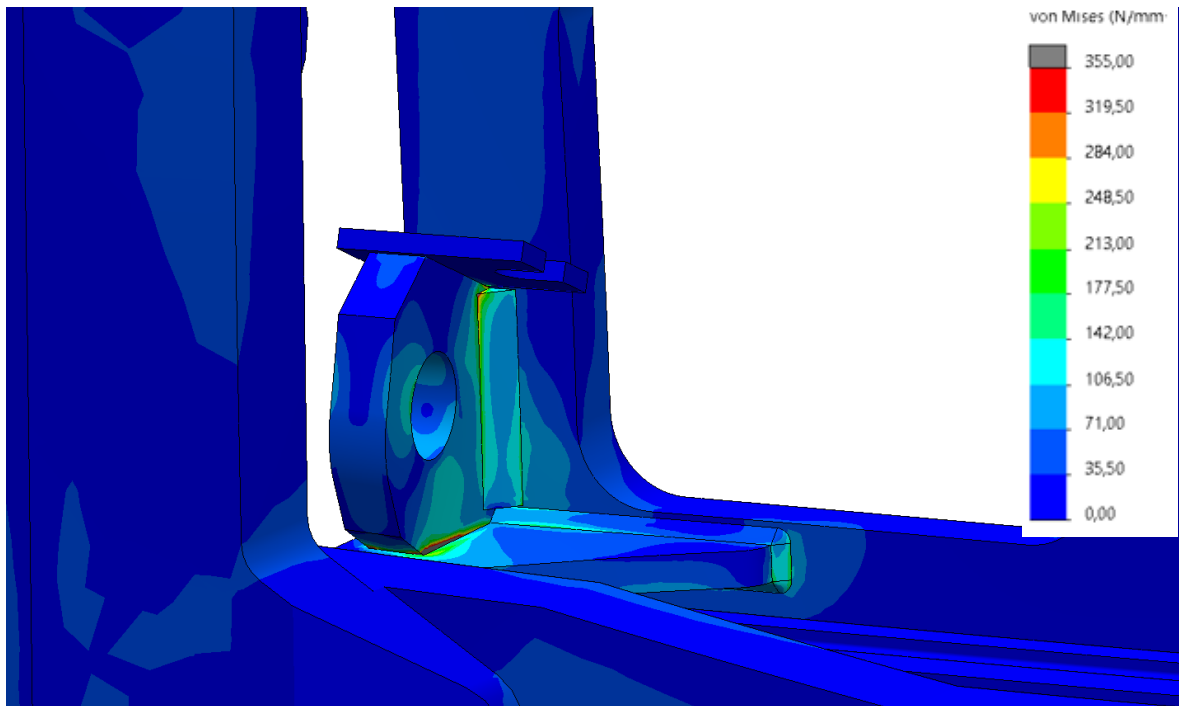


**Figure 47.** LC3 VonMises stresses at cylinder bracket.

The displacements from loading cases 2 and 3 are presented below.

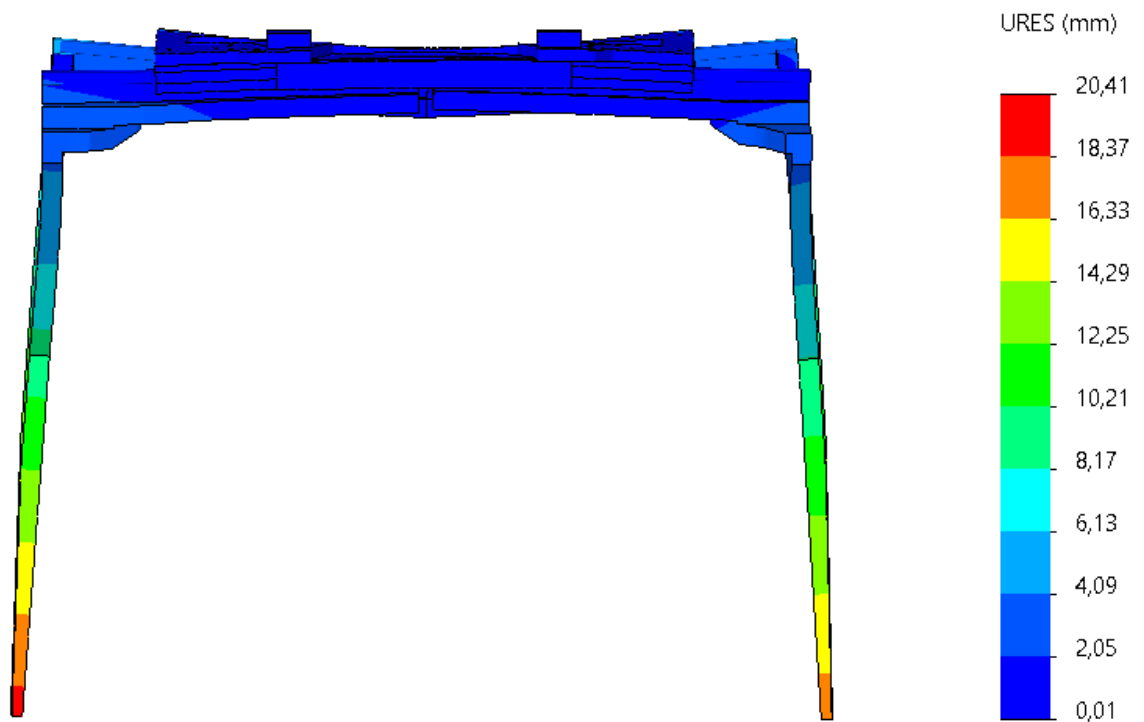


**Figure 48.** LC2 displacements from top, scaled 20 times.

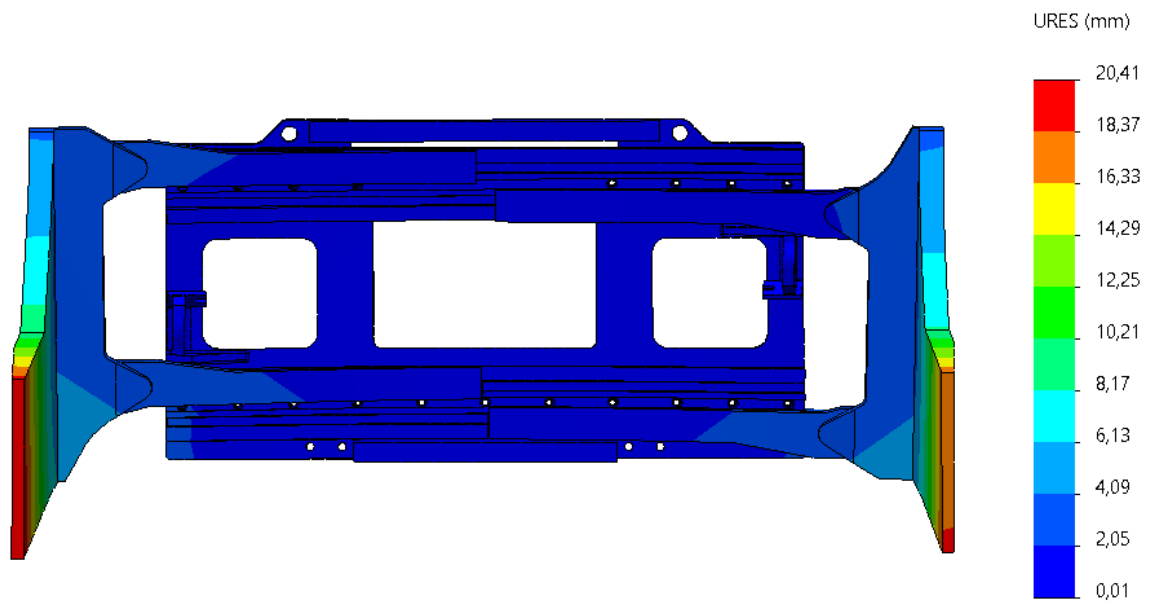


**Figure 49.** LC2 displacements from front, scaled 20 times.

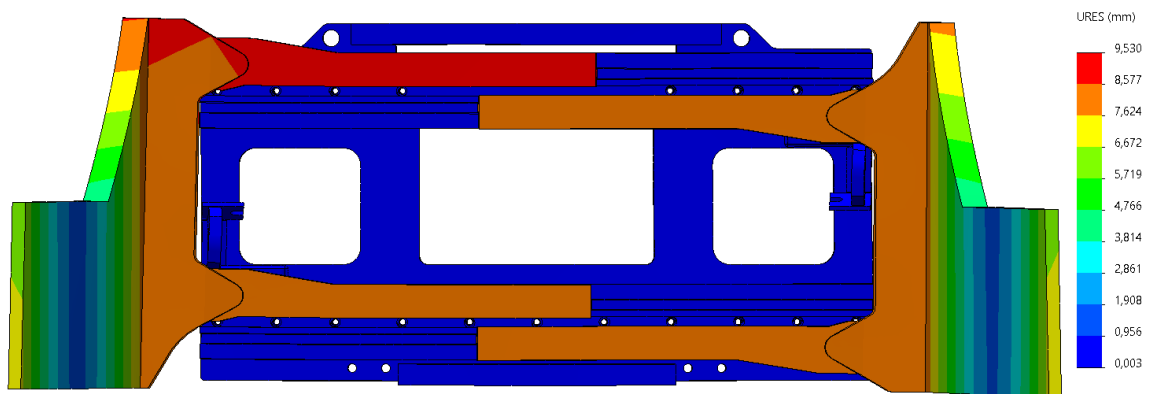


**Figure 50.** LC3 displacements from front, scaled 20 times.

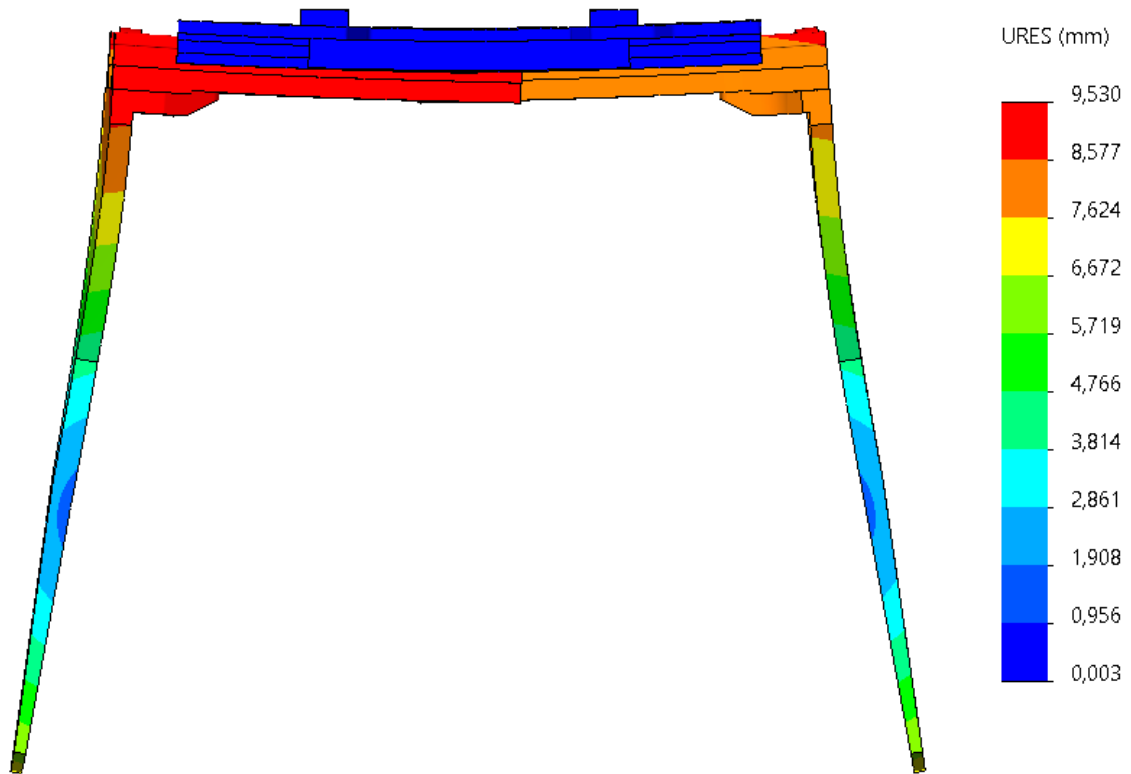


**Figure 51.** LC3 displacements from top, scaled 20 times.

The maximum displacements of both cases are presented below in table 8.

*Table 8. Maximum displacements in modified structure.*

Loading case	Maximum displacement [mm]	Frame plate maximum displacement
LC 2	20,4	2,5
LC 3	9,5	0,8

#### 4.4.1 Bolt forces

The bolt initial data stayed the same from the preliminary analyzes. The number of bolts stayed also the same and the dimensions how they are placed. The only difference here is the fact that between the aluminum profiles and the frame plate was added a 0,1 friction factor. The added friction factor doubled the analyzing time. All the bolt forces are listed in appendix II. The utilization ratio and factor of safety was also calculated here. The changes in the bolt forces were not significant. The shear force increased in some bolts but otherwise

the changes were minimal. This shows us again that the bolt is not the part that fails if the structure breaks in static loading. The range of the utilization ratio was between 24-31 %. This gives us again a factor of safety around four of the combined shear and tension forces.

#### 4.5 Fatigue life results

In this chapter the fatigue analysis results are presented both the bolts and the frame plate. The calculations were done according to the methods presented earlier. The calculations are estimations for the fatigue life and not absolute results.

##### 4.5.1 Frame plate fatigue life results

The fatigue life for the frame plate is presented in this chapter. The more critical point in the frame plate fatigue life is the cylinder bracket. More precisely the weld by the bracket. The Hot Spot stresses were calculated from two point as presented earlier. All in all, four Hot spot stresses were calculated because the clamping and the clamping and lifting was calculated separately. The calculations of the Hot Spot stresses are presented in appendix III-VI. The stress distributions (including all components) through the thickness of the plates are presented below in figure 52-55.  $x = 0$  in the start of the graph.

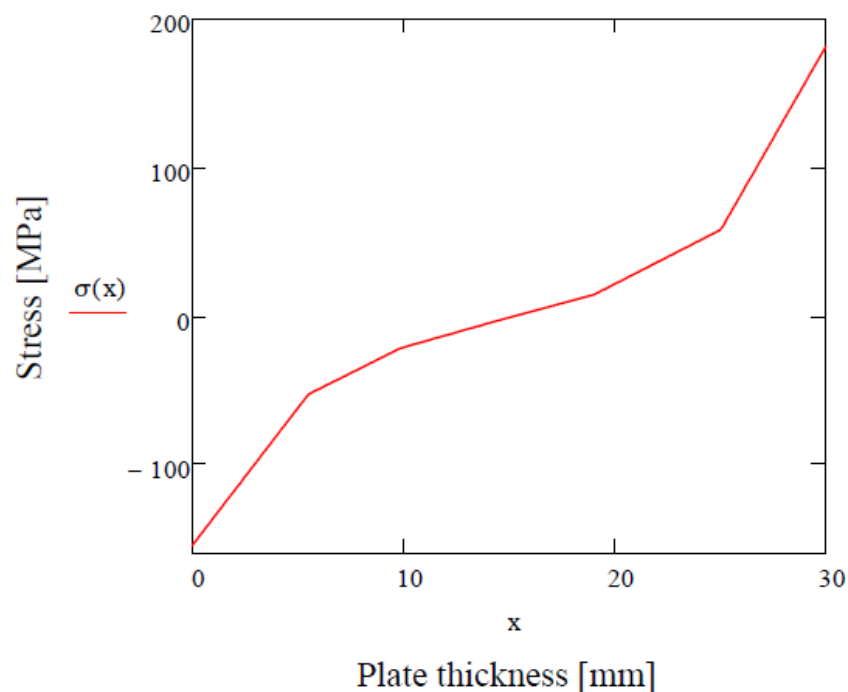


**Figure 52.** Stress through the thickness in cylinder bracket, only clamping.

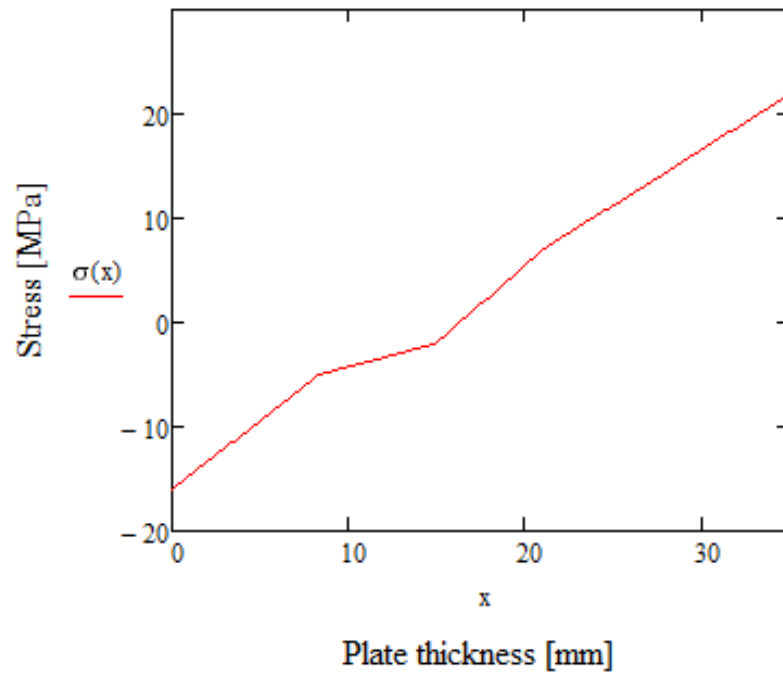


**Figure 53.** Stress through the thickness in frame plate, only clamping.

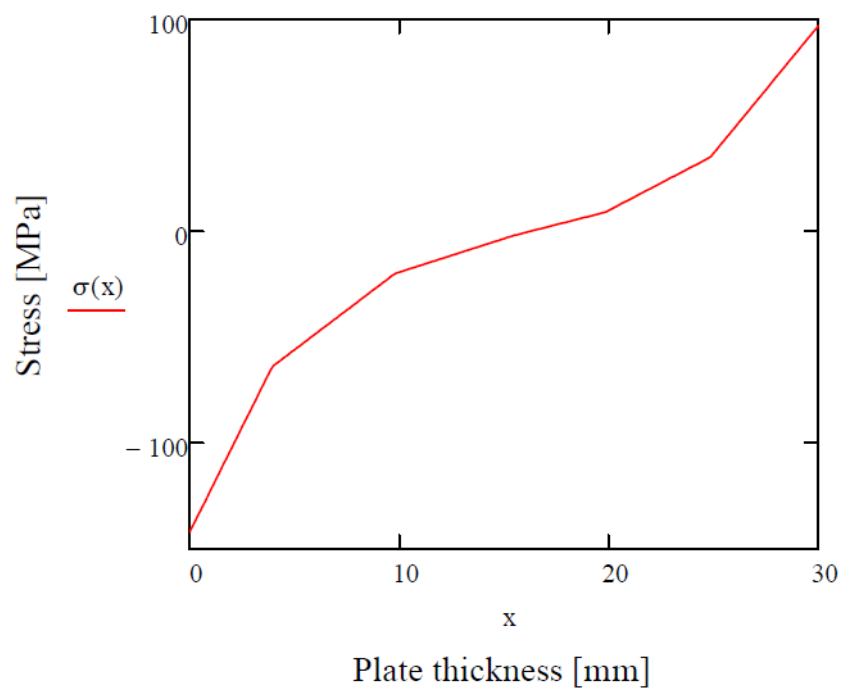


**Figure 54.** Stress through the thickness in cylinder bracket, clamping and lifting.

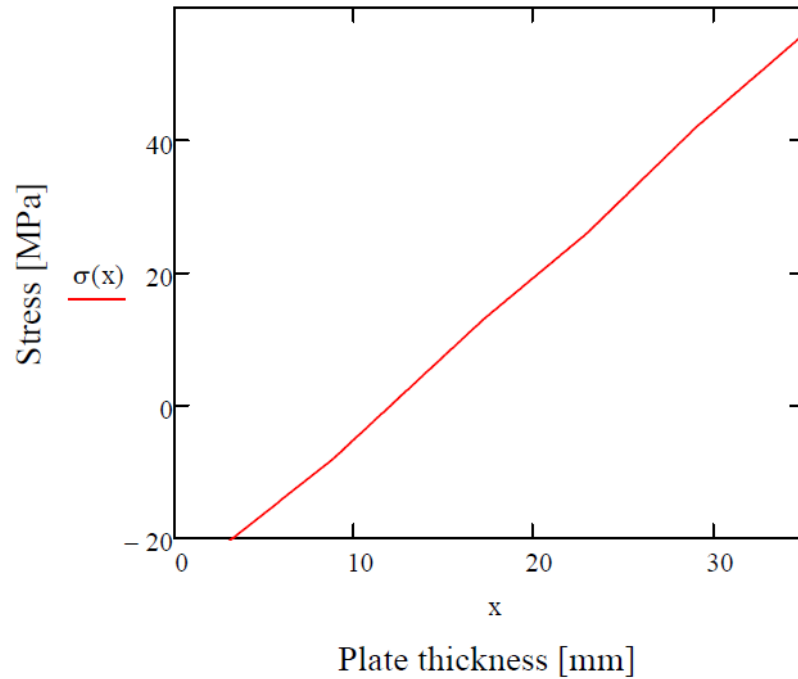


**Figure 55.** Stress through the thickness in frame plate, only clamping.

The calculated Hot Spot stresses are presented below in table 9.

*Table 9. Hot Spot stress results.*

Loading type	Membrane stress [MPa]	Bending stress [MPa]	Structural stress [MPa]
Clamping, cylinder bracket	1	-121	-119
Clamping, frame plate	3	-19	-15
Clamping and lifting, cylinder bracket	-8	-87	-95
Clamping and lifting, frame plate	14	-42	-28

The fatigue life was calculated using the calculated structural stresses that gave us the stress range. The calculated fatigue life is presented below in table 10.

*Table 10. Fatigue life results for frame plate.*

	$N_D$ [cycles]
Cylinder bracket	600 665
Frame plate	44 515 500

#### 4.5.2 Bolt fatigue life results

The fatigue life calculation excel sheets for the bolts are in appendix VII and VIII. The most critical bolts are presented here and the calculated estimate for the fatigue life. The same analyses to determine the stress range was used as for the frame plate and cylinder bracket calculations. The estimated fatigue life for the most critical bolts is presented below in table 11.

*Table 11. Bolt fatigue life results for most critical bolts.*

Bolt number	$N_D$ [cycles]
3	1 786 513
6	767 798
14	1 037 740

## 5 DISCUSSION

In this chapter the results will be discussed and about the process of the calculations. The preliminary analyzes took roughly 3 hours per analysis. The number of elements was not that much but the big contact areas with the virtual walls rose the calculation times a lot. The four different loading cases was provided by Auramo which were used to find the critical spot in the bale clamp and where the structure would fail. The critical spots in the structure were the cylinder bracket and the bolted connections between the aluminum profiles and the frame plate. From the results of the preliminary analyses some improvements to the structure were made and the two most critical loading cases were analyzed once again using more finer mesh on certain parts. Loading case two and three was chosen here. Loading case three was chosen also because it caused the biggest stress variations of the cases where only clamping was done.

The bolts were analyzed using Solidworks FEA bolted connection tools. This made it possible to easily apply the given tightening torque and the bolt strength properties. A bolt force diagram was made from one bolt where the force and strains are shown. The static and fatigue life calculations were done using data got from the FE-analysis and equations from Eurocode 3. The results showed that the bolts are not close to failure caused by the static loading. The utilization ratio was in the bolts between 24-32 %. The big risk of failure comes from the loading that causes fatigue. The estimated fatigue life for each bolt was calculated for the improved structure. From the calculations the most critical bolts were found. Bolt number six was the most critical one where the estimated fatigue life was 767 798 cycles. This can be easily increased by adding the amount of tightening torque which lower the stress variation in the bolt.

The other critical part in the structure was the area at the cylinder bracket. The force from the cylinder to the bracket in combination with the vertical force of the arms the plate was subjected to heavy bending. Loading case 2 caused the biggest stresses on the plate and this was chosen for the fatigue calculations. The addition of the stiffeners decreased the stresses a lot. The stiffeners reduced the amount of bending in the frame plate caused by the cylinder bracket. Welds were also added for calculating the fatigue life. The Hot Spot stress method

was used for the calculations. The Hot Spot stress was calculated by the weld toe of the cylinder bracket and the frame plate from which the toe at the bracket was more critical. The estimated fatigue life at the bracket was 600 665 cycles.

The model being so complex with the big contact areas there is always some uncertainties. In this study only the case where the arms are centered was investigated. The arms can also be uncentered because they can move the bale when clamped sideways. There can also be some excessive forces that the bale clamp can be under. There can be some bumps that the forklift can drive into under operation (uneven drive platform) or the clamping is uneven and the forces go not the most efficient way through the structure.

The research was done using analytical equations and FE-analysis. The results should be verified and checked using practical tests in a laboratory. But from the basis of these analyses the capacity could be increased. Some further improvements could be made on basis of the results when the critical spots are now known.

## 6 SUMMARY

This master's thesis objective was to find out if the capacity of a bale lamp could be increased with the given limitations. The thesis was done to Auramo which is one of the leading forklift fork and attachment manufacturers in the world. The focus was on the FE-modelling and to get liable results from it. Four loading cases were analyzed from which two was taken for more closer inspection.

From the closer inspections an estimated fatigue life was gotten for the structure and the limiting factor for the capacity increase was found. The FE-model was complex due to the fact it has so moving parts and a complex geometry. The results are not absolute, and they should be verified using laboratory tests. Also, the objective was to find the critical spot/limiting factor for increasing the capacity and it was done successfully.

**LIST OF REFERENCES**

Bolzoni Group 2021a. [Referred 25.1.2021]. Available:

<https://en.bolzonigroup.com/prodotto.php?p=50>

Hobbacher, A. 2014. Recommendations for fatigue design of welded joints and components. IIW-document XIII-2460-13/XV-1440-13. 164 p.

Jonsson, B., Doubmann, G., Hobbacher, A., Kassner, M., Marquis, G. 2016. IIW Guidelines on Weld Quality in Relationship to Fatigue Strength. Springer Nature. 115p.

Virtanen, J. 2021. Loading cases [private email]. Receiver: Mikael Paavolainen. Sent 26.3.2021 at 16:36 (GMT +0200).

SFS EN ISO 898-1. 2013. Mechanical properties of fasteners made of carbon steel and alloy steel. Part 2. Nuts with specified property classes. Coarse thread and fine pitch thread. Helsinki: Finnish Standards association. 68 p.

SFS-EN 1993-1-8. 2005. Eurocode 3. Teräsrakenteiden suunnittelu. Osa 1-8: Liitosten mitoitus. Helsinki: Suomen standardoimisliitto. p. 148.

Matikainen, A. 2013. Solidworks simulations and Femap FEA-comparison using rectangular hollow section beams. 48 p. Available: <https://lutpub.lut.fi/handle/10024/93950>  
Referred: 3.7.2021

Niemi, E. & Kemppe, J. 1993. Hitsatun rakenteen suunnittelun perusteet. 1. painos. Helsinki: Painatuskeskus. 337 p.

## Original structure, bolt forces

Loading case 1							
Type	X-Component	Y-Component	Z-Component	Resultant	Connector	UR	Factor of safety
Shear Force (N)	2,0657	322,26	0	322,27	Counterbore Screw-1	0,25	4,06
Axial Force (N)	0	0	46792	46792	Counterbore Screw-1		
Shear Force (N)	96,771	413,8	0	424,97	Counterbore Screw-2	0,24	4,22
Axial Force (N)	0	0	44692	44692	Counterbore Screw-2		
Shear Force (N)	283,25	577,55	0	643,27	Counterbore Screw-3	0,26	3,90
Axial Force (N)	0	0	47851	47851	Counterbore Screw-3		
Shear Force (N)	-33,259	978,46	0	979,03	Counterbore Screw-4	0,25	3,95
Axial Force (N)	0	0	46469	46469	Counterbore Screw-4		
Shear Force (N)	-112,95	164,57	0	199,6	Counterbore Screw-5	0,25	4,01
Axial Force (N)	0	0	47648	47648	Counterbore Screw-5		
Shear Force (N)	-154,51	-139,57	0	208,22	Counterbore Screw-6	0,24	4,23
Axial Force (N)	0	0	45157	45157	Counterbore Screw-6		
Shear Force (N)	-287,82	-395,43	0	489,08	Counterbore Screw-7	0,24	4,09
Axial Force (N)	0	0	45928	45928	Counterbore Screw-7		
Shear Force (N)	-233,91	-711,65	0	749,11	Counterbore Screw-8	0,25	4,08
Axial Force (N)	0	0	45446	45446	Counterbore Screw-8		
Shear Force (N)	-692,3	-1246,4	0	1425,8	Counterbore Screw-9	0,26	3,86
Axial Force (N)	0	0	46423	46423	Counterbore Screw-9		
Shear Force (N)	-1000,9	-660,81	0	1199,3	Counterbore Screw-10	0,27	3,74
Axial Force (N)	0	0	48560	48560	Counterbore Screw-10		
Shear Force (N)	-940,72	-250,2	0	973,43	Counterbore Screw-11	0,25	4,01
Axial Force (N)	0	0	45749	45749	Counterbore Screw-11		
Shear Force (N)	-764,53	122,82	0	774,34	Counterbore Screw-12	0,25	4,08
Axial Force (N)	0	0	45404	45404	Counterbore Screw-12		
Shear Force (N)	-640,45	202,47	0	671,7	Counterbore Screw-13	0,24	4,09
Axial Force (N)	0	0	45554	45554	Counterbore Screw-13		
Shear Force (N)	-84,825	119,13	-7,28E-12	146,25	Counterbore Screw-14	0,26	3,88
Axial Force (N)	-6,04E-09	0	49416	49416	Counterbore Screw-14		
Shear Force (N)	400,36	-11,314	0	400,52	Counterbore Screw-15	0,24	4,14
Axial Force (N)	0	0	45654	45654	Counterbore Screw-15		
Shear Force (N)	496,19	-9,5073	0	496,28	Counterbore Screw-16	0,24	4,10
Axial Force (N)	0	0	45811	45811	Counterbore Screw-16		
Shear Force (N)	647,56	28,468	0	648,18	Counterbore Screw-17	0,25	4,08
Axial Force (N)	0	0	45717	45717	Counterbore Screw-17		
Shear Force (N)	754,1	149,67	0	768,81	Counterbore Screw-18	0,25	4,04
Axial Force (N)	0	0	45828	45828	Counterbore Screw-18		
Shear Force (N)	714,21	345,66	0	793,46	Counterbore Screw-19	0,25	4,06
Axial Force (N)	0	0	45512	45512	Counterbore Screw-19		

## Appendix I, 2

Loading case 2							
Type	X-Component	Y-Component	Z-Component	Resultant	Connector	UR	Factor of safety
Shear Force (N)	-296,93	203,53	0	359,99	Counterbore Screw-1	0,26	3,89
Axial Force (N)	0	0	48745	48745	Counterbore Screw-1		
Shear Force (N)	-889,7	1153,5	0	1456,8	Counterbore Screw-2	0,32	3,17
Axial Force (N)	0	0	57331	57331	Counterbore Screw-2		
Shear Force (N)	-1213,5	1251,4	0	1743,1	Counterbore Screw-3	0,29	3,46
Axial Force (N)	0	0	51340	51340	Counterbore Screw-3		
Shear Force (N)	-1291,3	1628,1	0	2078	Counterbore Screw-4	0,28	3,54
Axial Force (N)	0	0	49320	49320	Counterbore Screw-4		
Shear Force (N)	78,804	-481,22	0	487,63	Counterbore Screw-5	0,26	3,80
Axial Force (N)	0	0	49531	49531	Counterbore Screw-5		
Shear Force (N)	569,37	-263,56	0	627,41	Counterbore Screw-6	0,32	3,13
Axial Force (N)	0	0	60080	60080	Counterbore Screw-6		
Shear Force (N)	785,02	-162,4	0	801,65	Counterbore Screw-7	0,27	3,65
Axial Force (N)	0	0	50913	50913	Counterbore Screw-7		
Shear Force (N)	525,81	106,8	0	536,54	Counterbore Screw-8	0,26	3,92
Axial Force (N)	0	0	47902	47902	Counterbore Screw-8		
Shear Force (N)	-2131,3	2102,8	0	2994	Counterbore Screw-9	0,28	3,57
Axial Force (N)	0	0	46610	46610	Counterbore Screw-9		
Shear Force (N)	-2718,5	1751	0	3233,6	Counterbore Screw-10	0,32	3,17
Axial Force (N)	0	0	52797	52797	Counterbore Screw-10		
Shear Force (N)	-2661,1	1526,1	0	3067,7	Counterbore Screw-11	0,28	3,57
Axial Force (N)	0	0	46369	46369	Counterbore Screw-11		
Shear Force (N)	-1768	1172,4	0	2121,3	Counterbore Screw-12	0,26	3,82
Axial Force (N)	0	0	45231	45231	Counterbore Screw-12		
Shear Force (N)	-1720,2	-162,63	0	1727,9	Counterbore Screw-13	0,26	3,78
Axial Force (N)	0	0	46670	46670	Counterbore Screw-13		
Shear Force (N)	-475,63	-808,97	-5,82E-11	938,43	Counterbore Screw-14	0,32	3,17
Axial Force (N)	-7,16E-09	0	58581	58581	Counterbore Screw-14		
Shear Force (N)	730,45	-307,17	0	792,4	Counterbore Screw-15	0,26	3,77
Axial Force (N)	0	0	49154	49154	Counterbore Screw-15		
Shear Force (N)	755,45	244,92	0	794,16	Counterbore Screw-16	0,25	3,96
Axial Force (N)	0	0	46773	46773	Counterbore Screw-16		
Shear Force (N)	1108,9	173,1	0	1122,3	Counterbore Screw-17	0,26	3,90
Axial Force (N)	0	0	46702	46702	Counterbore Screw-17		
Shear Force (N)	1281,6	330,51	0	1323,6	Counterbore Screw-18	0,26	3,79
Axial Force (N)	0	0	47637	47637	Counterbore Screw-18		
Shear Force (N)	1049,6	596,68	0	1207,4	Counterbore Screw-19	0,26	3,89
Axial Force (N)	0	0	46624	46624	Counterbore Screw-19		

Appendix I, 3

Loading case 3							
Type	X-Component	Y-Component	Z-Component	Resultant	Connector	UR	Factor of safety
Shear Force (N)	6,2412	291,3	0	291,37	Counterbore Screw-1	0,25	4,01
Axial Force (N)	0	0	47469	47469	Counterbore Screw-1		
Shear Force (N)	66,966	124,15	0	141,06	Counterbore Screw-2	0,23	4,28
Axial Force (N)	0	0	44753	44753	Counterbore Screw-2		
Shear Force (N)	287,02	64,129	0	294,1	Counterbore Screw-3	0,25	3,96
Axial Force (N)	0	0	48071	48071	Counterbore Screw-3		
Shear Force (N)	-16,822	180,59	0	181,37	Counterbore Screw-4	0,24	4,08
Axial Force (N)	0	0	46817	46817	Counterbore Screw-4		
Shear Force (N)	-17,572	-52,619	0	55,475	Counterbore Screw-5	0,25	3,98
Axial Force (N)	0	0	48340	48340	Counterbore Screw-5		
Shear Force (N)	2,1039	-203,95	0	203,96	Counterbore Screw-6	0,24	4,21
Axial Force (N)	0	0	45324	45324	Counterbore Screw-6		
Shear Force (N)	-117,68	-194,26	0	227,13	Counterbore Screw-7	0,24	4,13
Axial Force (N)	0	0	46174	46174	Counterbore Screw-7		
Shear Force (N)	-83,581	-210,02	0	226,04	Counterbore Screw-8	0,24	4,18
Axial Force (N)	0	0	45631	45631	Counterbore Screw-8		
Shear Force (N)	-636,69	-399,27	0	751,53	Counterbore Screw-9	0,25	3,97
Axial Force (N)	0	0	46742	46742	Counterbore Screw-9		
Shear Force (N)	-963,23	-145,78	0	974,2	Counterbore Screw-10	0,27	3,77
Axial Force (N)	0	0	48731	48731	Counterbore Screw-10		
Shear Force (N)	-897,31	-22,089	0	897,59	Counterbore Screw-11	0,25	4,01
Axial Force (N)	0	0	45864	45864	Counterbore Screw-11		
Shear Force (N)	-758,96	109,23	0	766,78	Counterbore Screw-12	0,25	4,07
Axial Force (N)	0	0	45503	45503	Counterbore Screw-12		
Shear Force (N)	-707,18	52,563	0	709,13	Counterbore Screw-13	0,24	4,09
Axial Force (N)	0	0	45464	45464	Counterbore Screw-13		
Shear Force (N)	-118,87	44,512	-1,46E-11	126,93	Counterbore Screw-14	0,25	3,92
Axial Force (N)	-5,97E-09	0	48877	48877	Counterbore Screw-14		
Shear Force (N)	245,92	97,487	0	264,54	Counterbore Screw-15	0,24	4,17
Axial Force (N)	0	0	45684	45684	Counterbore Screw-15		
Shear Force (N)	259,94	127,72	0	289,62	Counterbore Screw-16	0,24	4,14
Axial Force (N)	0	0	45935	45935	Counterbore Screw-16		
Shear Force (N)	390,79	101,5	0	403,76	Counterbore Screw-17	0,24	4,12
Axial Force (N)	0	0	45819	45819	Counterbore Screw-17		
Shear Force (N)	519,25	115,86	0	532,02	Counterbore Screw-18	0,25	4,07
Axial Force (N)	0	0	46056	46056	Counterbore Screw-18		
Shear Force (N)	467,18	141,68	0	488,19	Counterbore Screw-19	0,24	4,10
Axial Force (N)	0	0	45874	45874	Counterbore Screw-19		

Appendix I, 4

Loading case 4							
Type	X-Component	Y-Component	Z-Component	Resultant	Connector	UR	Factor of safety
Shear Force (N)	2,0657	322,26	0	322,27	Counterbore Screw-1	0,25	4,06
Axial Force (N)	0	0	46792	46792	Counterbore Screw-1		
Shear Force (N)	96,771	413,8	0	424,97	Counterbore Screw-2	0,24	4,22
Axial Force (N)	0	0	44692	44692	Counterbore Screw-2		
Shear Force (N)	283,25	577,55	0	643,27	Counterbore Screw-3	0,26	3,90
Axial Force (N)	0	0	47851	47851	Counterbore Screw-3		
Shear Force (N)	-33,259	978,46	0	979,03	Counterbore Screw-4	0,25	3,95
Axial Force (N)	0	0	46469	46469	Counterbore Screw-4		
Shear Force (N)	-112,95	164,57	0	199,6	Counterbore Screw-5	0,25	4,01
Axial Force (N)	0	0	47648	47648	Counterbore Screw-5		
Shear Force (N)	-154,51	-139,57	0	208,22	Counterbore Screw-6	0,24	4,23
Axial Force (N)	0	0	45157	45157	Counterbore Screw-6		
Shear Force (N)	-287,82	-395,43	0	489,08	Counterbore Screw-7	0,24	4,09
Axial Force (N)	0	0	45928	45928	Counterbore Screw-7		
Shear Force (N)	-233,91	-711,65	0	749,11	Counterbore Screw-8	0,25	4,08
Axial Force (N)	0	0	45446	45446	Counterbore Screw-8		
Shear Force (N)	-692,3	-1246,4	0	1425,8	Counterbore Screw-9	0,26	3,86
Axial Force (N)	0	0	46423	46423	Counterbore Screw-9		
Shear Force (N)	-1000,9	-660,81	0	1199,3	Counterbore Screw-10	0,27	3,74
Axial Force (N)	0	0	48560	48560	Counterbore Screw-10		
Shear Force (N)	-940,72	-250,2	0	973,43	Counterbore Screw-11	0,25	4,01
Axial Force (N)	0	0	45749	45749	Counterbore Screw-11		
Shear Force (N)	-764,53	122,82	0	774,34	Counterbore Screw-12	0,25	4,08
Axial Force (N)	0	0	45404	45404	Counterbore Screw-12		
Shear Force (N)	-640,45	202,47	0	671,7	Counterbore Screw-13	0,24	4,09
Axial Force (N)	0	0	45554	45554	Counterbore Screw-13		
Shear Force (N)	-84,825	119,13	-7,28E-12	146,25	Counterbore Screw-14	0,26	3,88
Axial Force (N)	-6,04E-09	0	49416	49416	Counterbore Screw-14		
Shear Force (N)	400,36	-11,314	0	400,52	Counterbore Screw-15	0,24	4,14
Axial Force (N)	0	0	45654	45654	Counterbore Screw-15		
Shear Force (N)	496,19	-9,5073	0	496,28	Counterbore Screw-16	0,24	4,10
Axial Force (N)	0	0	45811	45811	Counterbore Screw-16		
Shear Force (N)	647,56	28,468	0	648,18	Counterbore Screw-17	0,25	4,08
Axial Force (N)	0	0	45717	45717	Counterbore Screw-17		
Shear Force (N)	754,1	149,67	0	768,81	Counterbore Screw-18	0,25	4,04
Axial Force (N)	0	0	45828	45828	Counterbore Screw-18		
Shear Force (N)	714,21	345,66	0	793,46	Counterbore Screw-19	0,25	4,06
Axial Force (N)	0	0	45512	45512	Counterbore Screw-19		

**Modified structure, bolt forces**

Loading case 2							
Type	X-Component	Y-Component	Z-Component	Resultant	Connector	UR	Factor of safety
Shear Force (N)	590,29	-196,93	0	622,27	Counterbore Screw-1	0,24	4,09
Axial Force (N)	0	0	-45641	45641	Counterbore Screw-1		
Shear Force (N)	925,58	179,13	0	942,76	Counterbore Screw-2	0,25	3,94
Axial Force (N)	0	0	-46596	46596	Counterbore Screw-2		
Shear Force (N)	792,3	450,75	0	911,55	Counterbore Screw-3	0,29	3,45
Axial Force (N)	0	0	-53724	53724	Counterbore Screw-3		
Shear Force (N)	246,39	761,4	0	800,27	Counterbore Screw-4	0,24	4,11
Axial Force (N)	0	0	-44980	44980	Counterbore Screw-4		
Shear Force (N)	-454,82	-256,06	0	521,95	Counterbore Screw-5	0,24	4,11
Axial Force (N)	0	0	-45614	45614	Counterbore Screw-5		
Shear Force (N)	-1065,3	-1021,1	0	1475,6	Counterbore Screw-6	0,31	3,21
Axial Force (N)	0	0	-56374	56374	Counterbore Screw-6		
Shear Force (N)	-1456,7	-1473,3	0	2071,8	Counterbore Screw-7	0,28	3,52
Axial Force (N)	0	0	-49561	49561	Counterbore Screw-7		
Shear Force (N)	-1374,6	-2220,1	0	2611,2	Counterbore Screw-8	0,27	3,71
Axial Force (N)	0	0	-45392	45392	Counterbore Screw-8		
Shear Force (N)	1778	-1523,9	0	2341,8	Counterbore Screw-9	0,26	3,82
Axial Force (N)	0	0	-44586	44586	Counterbore Screw-9		
Shear Force (N)	1837,5	-1024	0	2103,6	Counterbore Screw-10	0,26	3,82
Axial Force (N)	0	0	-45303	45303	Counterbore Screw-10		
Shear Force (N)	1624,7	-609,83	0	1735,4	Counterbore Screw-11	0,25	3,94
Axial Force (N)	0	0	-44617	44617	Counterbore Screw-11		
Shear Force (N)	995,54	-299,32	0	1039,6	Counterbore Screw-12	0,24	4,13
Axial Force (N)	0	0	-44128	44128	Counterbore Screw-12		
Shear Force (N)	690,32	388,11	0	791,94	Counterbore Screw-13	0,26	3,80
Axial Force (N)	0	0	-48775	48775	Counterbore Screw-13		
Shear Force (N)	-533,11	638,17	0	831,54	Counterbore Screw-14	0,30	3,36
Axial Force (N)	0	0	-55342	55342	Counterbore Screw-14		
Shear Force (N)	-1760,1	-419,57	0	1809,4	Counterbore Screw-15	0,26	3,92
Axial Force (N)	0	0	-44700	44700	Counterbore Screw-15		
Shear Force (N)	-2082,9	-2032,9	0	2910,6	Counterbore Screw-16	0,26	3,84
Axial Force (N)	0	0	-42956	42956	Counterbore Screw-16		
Shear Force (N)	-3092,9	-3001,4	0	4309,8	Counterbore Screw-17	0,29	3,45
Axial Force (N)	0	0	-45125	45125	Counterbore Screw-17		
Shear Force (N)	-3094,8	-3566,4	0	4722	Counterbore Screw-18	0,31	3,20
Axial Force (N)	0	0	-48351	48351	Counterbore Screw-18		
Shear Force (N)	-2814,2	-4089,3	0	4964,1	Counterbore Screw-19	0,29	3,47
Axial Force (N)	0	0	-43179	43179	Counterbore Screw-19		

## Appendix II, 2

Loading case 3							
Type	X-Component	Y-Component	Z-Component	Resultant	Connector	UR	Factor of safety
Shear Force (N)	-279,95	319,07	0	424,48	Counterbore Screw-1	0,24	4,12
Axial Force (N)	0	0	-45825	45825	Counterbore Screw-1		
Shear Force (N)	761,37	-323,28	0	827,15	Counterbore Screw-2	0,28	3,57
Axial Force (N)	0	0	-52034	52034	Counterbore Screw-2		
Shear Force (N)	34,583	269,73	0	271,94	Counterbore Screw-3	0,24	4,25
Axial Force (N)	0	0	-44697	44697	Counterbore Screw-3		
Shear Force (N)	14,677	230,83	0	231,29	Counterbore Screw-4	0,25	3,97
Axial Force (N)	0	0	-48071	48071	Counterbore Screw-4		
Shear Force (N)	-17,227	-260,59	0	261,15	Counterbore Screw-5	0,25	4,02
Axial Force (N)	0	0	-47382	47382	Counterbore Screw-5		
Shear Force (N)	53,071	-81,763	0	97,477	Counterbore Screw-6	0,23	4,34
Axial Force (N)	0	0	-44225	44225	Counterbore Screw-6		
Shear Force (N)	179,82	-60,152	0	189,61	Counterbore Screw-7	0,25	4,07
Axial Force (N)	0	0	-46929	46929	Counterbore Screw-7		
Shear Force (N)	226,87	-191,94	0	297,17	Counterbore Screw-8	0,24	4,16
Axial Force (N)	0	0	-45681	45681	Counterbore Screw-8		
Shear Force (N)	957,94	-13,111	0	958,03	Counterbore Screw-9	0,25	4,02
Axial Force (N)	0	0	-45601	45601	Counterbore Screw-9		
Shear Force (N)	789,83	-70,965	0	793,01	Counterbore Screw-10	0,25	4,04
Axial Force (N)	0	0	-45739	45739	Counterbore Screw-10		
Shear Force (N)	616,55	-116,5	0	627,46	Counterbore Screw-11	0,24	4,08
Axial Force (N)	0	0	-45710	45710	Counterbore Screw-11		
Shear Force (N)	425,79	-121,06	0	442,67	Counterbore Screw-12	0,24	4,13
Axial Force (N)	0	0	-45597	45597	Counterbore Screw-12		
Shear Force (N)	319,5	-12,843	0	319,76	Counterbore Screw-13	0,24	4,14
Axial Force (N)	0	0	-45806	45806	Counterbore Screw-13		
Shear Force (N)	-127,11	120,39	0	175,07	Counterbore Screw-14	0,25	4,02
Axial Force (N)	0	0	-47640	47640	Counterbore Screw-14		
Shear Force (N)	-596,46	91,276	0	603,41	Counterbore Screw-15	0,24	4,11
Axial Force (N)	0	0	-45480	45480	Counterbore Screw-15		
Shear Force (N)	-643,54	-38,662	0	644,71	Counterbore Screw-16	0,24	4,12
Axial Force (N)	0	0	-45185	45185	Counterbore Screw-16		
Shear Force (N)	-821,98	46,62	0	823,3	Counterbore Screw-17	0,25	4,02
Axial Force (N)	0	0	-45918	45918	Counterbore Screw-17		
Shear Force (N)	-874,18	325,45	0	932,8	Counterbore Screw-18	0,26	3,86
Axial Force (N)	0	0	-47606	47606	Counterbore Screw-18		
Shear Force (N)	-953,67	805,81	0	1248,5	Counterbore Screw-19	0,25	3,96
Axial Force (N)	0	0	-45625	45625	Counterbore Screw-19		

**Mathcad base for Hot Spot, cylinder bracket, only clamping**

```
data := READPRN("Puristuskorva.txt")
```

$$\sigma_{\text{data}} := \text{data}^{(1)} = \begin{pmatrix} -155 \\ -53 \\ -22 \\ -6 \\ 14 \\ 58 \\ 181 \end{pmatrix} \quad x_{\text{data}} := \text{data}^{(0)} = \begin{pmatrix} 0 \\ 5.51 \\ 9.86 \\ 13.82 \\ 19.02 \\ 25.05 \\ 30 \end{pmatrix}$$

```
x := 0, 0.125..30   t := 30
```

$$\sigma(x) := \text{linterp}(x_{\text{data}}, \sigma_{\text{data}}, x)$$

**STRESS COMPONENTS**

TTWT Method

$$\sigma_{\text{m}} := \frac{1}{t} \cdot \int_0^t \sigma(x) \, dx = 1.26$$

$$\sigma_{\text{b}} := \frac{6}{t^2} \cdot \int_0^t (\sigma(x) - \sigma_{\text{m}}) \cdot \left(\frac{t}{2} - x\right) \, dx = -120.72373$$

$$\sigma_{\text{HS}} := \sigma_{\text{b}} + \sigma_{\text{m}} = -119.463$$

**Mathcad base for Hot Spot, frame plate, only clamping**

```
data := READPRN("Puristuslevy.txt")
```

$$\sigma_{\text{data}} := \text{data}^{(1)} = \begin{pmatrix} -16 \\ -5 \\ -2 \\ 7 \\ 14 \\ 22 \end{pmatrix}$$

$$x_{\text{data}} := \text{data}^{(0)} = \begin{pmatrix} 0 \\ 8.31 \\ 14.95 \\ 20.95 \\ 27.57 \\ 35 \end{pmatrix}$$

```
x := 0, 0.125..30    t := 35
```

$$\sigma(x) := \text{linterp}(x_{\text{data}}, \sigma_{\text{data}}, x)$$

**STRESS COMPONENTS**

TTWT Method

$$\sigma_{\text{m}} := \frac{1}{t} \cdot \int_0^t \sigma(x) \, dx = 3.079$$

$$\sigma_{\text{b}} := \frac{6}{t^2} \cdot \int_0^t (\sigma(x) - \sigma_{\text{m}}) \cdot \left(\frac{t}{2} - x\right) \, dx = -18.53768$$

$$\sigma_{\text{HS}} := \sigma_{\text{b}} + \sigma_{\text{m}} = -15.459$$

**Mathcad base for Hot Spot, cylinder bracket, clamping and lifting**

```
data := READPRN("Nostokorva.txt")
```

$$\sigma_{\text{data}} := \text{data}^{(1)} = \begin{pmatrix} -142 \\ -64 \\ -20 \\ -2 \\ 9 \\ 35 \\ 97 \end{pmatrix}$$

$$x_{\text{data}} := \text{data}^{(0)} = \begin{pmatrix} 0 \\ 3.93 \\ 9.79 \\ 15.46 \\ 19.83 \\ 24.85 \\ 30 \end{pmatrix}$$

```
x := 0, 0.125..30    t := 30
```

$$\sigma(x) := \text{linterp}(x_{\text{data}}, \sigma_{\text{data}}, x)$$

**STRESS COMPONENTS**

TTWT Method

$$\sigma_{\text{m}} := \frac{1}{t} \cdot \int_0^t \sigma(x) \, dx = -8.253$$

$$\sigma_{\text{b}} := \frac{6}{t^2} \cdot \int_0^t \left( \sigma(x) - \sigma_{\text{m}} \right) \cdot \left( \frac{t}{2} - x \right) \, dx = -86.57923$$

$$\sigma_{\text{HS}} := \sigma_{\text{b}} + \sigma_{\text{m}} = -94.833$$

**Mathcad base for Hot Spot, frame plate, clamping and lifting**

```
data := READPRN("Nostolevy.txt")
```

$$\sigma_{\text{data}} := \text{data}^{(1)} = \begin{pmatrix} -27 \\ -8 \\ 13 \\ 26 \\ 42 \\ 56 \end{pmatrix}$$

$$x_{\text{data}} := \text{data}^{(0)} = \begin{pmatrix} 0 \\ 8.84 \\ 17.18 \\ 22.94 \\ 29.01 \\ 35 \end{pmatrix}$$

```
x := 0, 0.125..30    t := 35
```

$$\sigma(x) := \text{linterp}(x_{\text{data}}, \sigma_{\text{data}}, x)$$

**STRESS COMPONENTS**

TTWT Method

$$\sigma_{\text{m}} := \frac{1}{t} \cdot \int_0^t \sigma(x) \, dx = 13.667$$

$$\sigma_{\text{b}} := \frac{6}{t^2} \cdot \int_0^t (\sigma(x) - \sigma_{\text{m}}) \cdot \left(\frac{t}{2} - x\right) \, dx = -42.10377$$

$$\sigma_{\text{HS}} := \sigma_{\text{b}} + \sigma_{\text{m}} = -28.436$$

Appendix VII,1

**Fatigue life calculations for bolts, LC2**

Only clamping								
Type	X-Componen	Y-Componen	Z-Componen	Resultant	Connector	$\sigma_D$	$\sigma$	Fatigue life
Shear Force (N)	-100,18	133,85	0	167,19	Counterbore Screw-1			
Axial Force (N)	0	0	-45761	45761	Counterbore Screw-1	-1,1974522	291,4713376	-1,45601E+11
Shear Force (N)	-9,118	154,23	0	154,5	Counterbore Screw-2		0,984076433	
Axial Force (N)	0	0	-45693	45693	Counterbore Screw-2	-0,7643312	291,0382166	-5,5988E+11
Shear Force (N)	114,19	176,62	0	210,32	Counterbore Screw-3		1,339617834	
Axial Force (N)	0	0	-45077	45077	Counterbore Screw-3	3,15923567	287,1146497	7928553050
Shear Force (N)	114,03	210,89	0	239,74	Counterbore Screw-4		1,527006369	
Axial Force (N)	0	0	-46905	46905	Counterbore Screw-4	-8,4840764	298,7579618	-409379688,7
Shear Force (N)	-30,059	-35,169	0	46,264	Counterbore Screw-5		0,294675159	
Axial Force (N)	0	0	-46708	46708	Counterbore Screw-5	-7,2292994	297,5031847	-661685139,8
Shear Force (N)	1,9181	-51,792	0	51,828	Counterbore Screw-6		0,33011465	
Axial Force (N)	0	0	-45756	45756	Counterbore Screw-6	-1,1656051	291,4394904	-1,57865E+11
Shear Force (N)	-48,197	74,335	0	88,593	Counterbore Screw-7		0,564286624	
Axial Force (N)	0	0	-47726	47726	Counterbore Screw-7	-13,713376	303,9872611	-96940861,84
Shear Force (N)	7,7383	-73,697	0	74,103	Counterbore Screw-8		0,471993631	
Axial Force (N)	0	0	-46000	46000	Counterbore Screw-8	-2,7197452	292,9936306	-12426686463
Shear Force (N)	285,46	-25,205	0	286,57	Counterbore Screw-9		1,825286624	
Axial Force (N)	0	0	-45941	45941	Counterbore Screw-9	-2,343949	292,6178344	-19413127634
Shear Force (N)	240,65	-85,286	0	255,31	Counterbore Screw-10		1,626178344	
Axial Force (N)	0	0	-45836	45836	Counterbore Screw-10	-1,6751592	291,9490446	-53182863903
Shear Force (N)	163,69	-127,34	0	207,39	Counterbore Screw-11		1,320955414	
Axial Force (N)	0	0	-46205	46205	Counterbore Screw-11	-4,0254777	294,2993631	-3832549132
Shear Force (N)	134,35	-84,166	0	158,54	Counterbore Screw-12		1,009808917	
Axial Force (N)	0	0	-46192	46192	Counterbore Screw-12	-3,9426752	294,2165605	-4079125046
Shear Force (N)	163,68	17,656	0	164,63	Counterbore Screw-13		1,048598726	
Axial Force (N)	0	0	-45670	45670	Counterbore Screw-13	-0,6178344	290,8917197	-1,06004E+12
Shear Force (N)	15,677	101,78	0	102,98	Counterbore Screw-14		0,655923567	
Axial Force (N)	0	0	-46184	46184	Counterbore Screw-14	-3,8917197	294,1656051	-4241459605
Shear Force (N)	-190,35	133,13	0	232,29	Counterbore Screw-15		1,47955414	
Axial Force (N)	0	0	-45610	45610	Counterbore Screw-15	-0,2356688	290,5095541	-1,91E+13
Shear Force (N)	-138,58	89,972	0	165,22	Counterbore Screw-16		1,052356688	
Axial Force (N)	0	0	-45560	45560	Counterbore Screw-16	0,08280255	290,1910828	4,40361E+14
Shear Force (N)	-196,17	90,422	0	216,01	Counterbore Screw-17		1,375859873	
Axial Force (N)	0	0	-46188	46188	Counterbore Screw-17	-3,9171975	294,1910828	-4159236528
Shear Force (N)	-130,2	122,53	0	178,79	Counterbore Screw-18		1,138789809	
Axial Force (N)	0	0	-47328	47328	Counterbore Screw-18	-11,178344	301,4522293	-178981277,5
Shear Force (N)	-140,83	134,42	0	194,68	Counterbore Screw-19		1,24	
Axial Force (N)	0	0	-45784	45784	Counterbore Screw-19	-1,343949	291,6178344	-1,02989E+11

## Appendix VII,2

Clamping and lifting									
Type	X-Component	Y-Component	Z-Component	Resultant	Connector	UR	$\sigma_D$	$\sigma$	Fatigue life
Shear Force (N)	590,29	-196,93	0	622,27	Counterbore Screw-1	0,24			
Axial Force (N)	0	0	-45641	45641	Counterbore Screw-1		-0,433121019	290,7070064	-3,0769E+12
Shear Force (N)	925,58	179,13	0	942,76	Counterbore Screw-2	0,25		6,004840764	
Axial Force (N)	0	0	-46596	46596	Counterbore Screw-2		-6,515923567	296,7898089	-903674578
Shear Force (N)	792,3	450,75	0	911,55	Counterbore Screw-3	0,29		5,806050955	
Axial Force (N)	0	0	-53724	53724	Counterbore Screw-3		-51,91719745	342,1910828	-1786513,43
Shear Force (N)	246,39	761,4	0	800,27	Counterbore Screw-4	0,24		5,097261146	
Axial Force (N)	0	0	-44980	44980	Counterbore Screw-4		3,777070064	286,4968153	4639539599
Shear Force (N)	-454,82	-256,06	0	521,95	Counterbore Screw-5	0,24		3,324522293	
Axial Force (N)	0	0	-45614	45614	Counterbore Screw-5		-0,261146497	290,5350318	-1,4037E+13
Shear Force (N)	-1065,3	-1021,1	0	1475,6	Counterbore Screw-6	0,31		9,398726115	
Axial Force (N)	0	0	-56374	56374	Counterbore Screw-6		-68,79617834	359,0700637	-767798,161
Shear Force (N)	-1456,7	-1473,3	0	2071,8	Counterbore Screw-7	0,28		13,19617834	
Axial Force (N)	0	0	-49561	49561	Counterbore Screw-7		-25,40127389	315,6751592	-15253640,9
Shear Force (N)	-1374,6	-2220,1	0	2611,2	Counterbore Screw-8	0,27		16,63184713	
Axial Force (N)	0	0	-45392	45392	Counterbore Screw-8		1,152866242	289,1210191	1,63156E+11
Shear Force (N)	1778	-1523,9	0	2341,8	Counterbore Screw-9	0,26		14,91592357	
Axial Force (N)	0	0	-44586	44586	Counterbore Screw-9		6,286624204	283,9872611	1006207402
Shear Force (N)	1837,5	-1024	0	2103,6	Counterbore Screw-10	0,26		13,39872611	
Axial Force (N)	0	0	-45303	45303	Counterbore Screw-10		1,719745223	288,5541401	49152733323
Shear Force (N)	1624,7	-609,83	0	1735,4	Counterbore Screw-11	0,25		11,05350318	
Axial Force (N)	0	0	-44617	44617	Counterbore Screw-11		6,089171975	284,1847134	1107299972
Shear Force (N)	995,54	-299,32	0	1039,6	Counterbore Screw-12	0,24		6,621656051	
Axial Force (N)	0	0	-44128	44128	Counterbore Screw-12		9,203821656	281,0700637	320653086,5
Shear Force (N)	690,32	388,11	0	791,94	Counterbore Screw-13	0,26		5,044203822	
Axial Force (N)	0	0	-48775	48775	Counterbore Screw-13		-20,39490446	310,6687898	-29469650,4
Shear Force (N)	-533,11	638,17	0	831,54	Counterbore Screw-14	0,30		5,296433121	
Axial Force (N)	0	0	-55342	55342	Counterbore Screw-14		-62,22292994	352,4968153	-1037740,19
Shear Force (N)	-1760,1	-419,57	0	1809,4	Counterbore Screw-15	0,26		11,52484076	
Axial Force (N)	0	0	-44700	44700	Counterbore Screw-15		5,560509554	284,7133758	1454106564
Shear Force (N)	-2082,9	-2032,9	0	2910,6	Counterbore Screw-16	0,26		18,5388535	
Axial Force (N)	0	0	-42956	42956	Counterbore Screw-16		16,66878981	273,6050955	53979368,31
Shear Force (N)	-3092,9	-3001,4	0	4309,8	Counterbore Screw-17	0,29		27,45095541	
Axial Force (N)	0	0	-45125	45125	Counterbore Screw-17		2,853503185	287,4203822	10759817963
Shear Force (N)	-3094,8	-3566,4	0	4722	Counterbore Screw-18	0,31		30,07643312	
Axial Force (N)	0	0	-48351	48351	Counterbore Screw-18		-17,69426752	307,9681529	-45127600,5
Shear Force (N)	-2814,2	-4089,3	0	4964,1	Counterbore Screw-19	0,29		31,61847134	
Axial Force (N)	0	0	-43179	43179	Counterbore Screw-19		15,24840764	275,0254777	70512567,37